Vibrations of the low energy states of toluene (1A1 and 1B2) and the toluene cation (2B1)

Adrian M. Gardner, Alistair M. Green, Victor M. Tamé-Reyes, Victoria H. K. Wilton, and Timothy G. Wright

Citation: J. Chem. Phys. **138**, 134303 (2013); doi: 10.1063/1.4796204
View online: http://dx.doi.org/10.1063/1.4796204
View Table of Contents: http://jcp.aip.org/resource/1/JCPSA6/v138/i13
Published by the American Institute of Physics.

Vibrations of the low energy states of toluene ($\tilde{X}\,^1A_1$ and $\tilde{A}\,^1B_2$) and the toluene cation ($\tilde{X}\,^2B_1$)

Adrian M. Gardner,[a] Alistair M. Green, Victor M. Tamé-Reyes, Victoria H. K. Wilton, and Timothy G. Wright[b]
School of Chemistry, University of Nottingham, University Park, Nottingham NG7 2RD, United Kingdom

(Received 23 December 2012; accepted 7 March 2013; published online 2 April 2013)

We commence by presenting an overview of the assignment of the vibrational frequencies of the toluene molecule in its ground (S_0) state. The assignment given is in terms of a recently proposed nomenclature, which allows the ring-localized vibrations to be compared straightforwardly across different monosubstituted benzenes. The frequencies and assignments are based not only on a range of previous work, but also on calculated wavenumbers for both the fully hydrogenated (toluene-h_8) and the deuterated-methyl group isotopologue (α_3-toluene-d_3), obtained from density functional theory (DFT), including artificial-isotope shifts. For the S_1 state, one-colour resonance-enhanced multiphoton ionization (REMPI) spectroscopy was employed, with the vibrational assignments also being based on previous work and time-dependent density functional theory (TDDFT) calculated values; but also making use of the activity observed in two-colour zero kinetic energy (ZEKE) spectroscopy. The ZEKE experiments were carried out employing a $(1 + 1')$ ionization scheme, using various vibrational levels of the S_1 state with an energy <630 cm^{-1} as intermediates; as such we only discuss in detail the assignment of the REMPI spectra at wavenumbers <700 cm^{-1}, referring to the assignment of the ZEKE spectra concurrently. Comparison of the ZEKE spectra for the two toluene isotopologues, as well as with previously reported dispersed-fluorescence spectra, and with the results of DFT calculations, provide insight both into the assignment of the vibrations in the S_1 and $D_0{}^+$ states, as well as the couplings between these vibrations. In particular, insight into the nature of a complicated Fermi resonance feature at $\sim$460 cm^{-1} in the S_1 state is obtained, and Fermi resonances in the cation are identified. Finally, we compare activity observed in both REMPI and ZEKE spectroscopy for both toluene isotopologues with that for fluorobenzene and chlorobenzene.
 [http://dx.doi.org/10.1063/1.4796204]

I. INTRODUCTION

Toluene (methylbenzene) is a familiar molecule to chemists, and has received much attention from spectroscopists, being the simplest substituted benzene to contain a methyl group. It formally possesses 39 normal vibrational modes, although one of these is more properly considered as an internal rotation, or "torsion," of the methyl group. In the ground electronic state, frequencies for all of these vibrational modes have been reported, and these will be discussed in detail below.

In a previous paper, we introduced a vibrational mode labelling scheme for the non-substituent-localized vibrations of the monosubstituted benzenes.[1] This scheme treats the substituent as a point mass and allows the identification of the ring-localized vibrations by a label, $\mathscr{M}_i$, where the label indicates the vibration of fluorobenzene which most closely resembles the monosubstituted benzene vibration: this can be done "by eye," or via a Duschinsky matrix approach—the reader is referred to Ref. 1 for further details. (The substituent-localized vibrations are assumed not to interact with the ring vibrations to a first approximation.) We noted therein,[1] that this new labelling scheme was more useful than the Wilson, Varsányi or Mulliken approaches (see below), since the label more obviously indicates the actual motion of the atoms, and also the same vibration has the same label, regardless of the substituent, even if the symmetry of the molecule changes. These aspects are exemplified in the present case. First, some of the vibrational modes of toluene are methyl-localized vibrations, and have frequencies which fall between the other vibrations, and so affect the Mulliken numbering scheme. This means a particular mode of toluene cannot easily be identified with the corresponding mode of another substituted benzene molecule purely on the basis of the Mulliken label. Additionally, it is common practice to assume that the CH_3 group is a point mass, and so to consider the molecule as having C_{2v} point group symmetry; this again causes uncertainty in how to label the modes under a Mulliken scheme, since the molecule is more properly considered as C_s symmetry and different point groups lead to different numbering. Finally, as noted previously by us[1] and others, the vibrations of the monosubstituted benzenes are quite different from those of benzene in a significant number of cases, making it difficult or even impossible to assign a single Wilson label to the mode. Our labelling scheme overcomes all of these drawbacks, allowing the vibrational motion to be deduced from the label, and also allowing direct comparison

[a]Present address: Chemistry Building, Department of Chemistry, Emory University, Atwood Hall 410, Atlanta, Georgia 30322, USA.
[b]Tim.Wright@nottingham.ac.uk

of vibrational activity with other monosubstituted benzenes, since the same ring-localized motions have the same label. Once the ring-localized vibrations have been assigned, then the substituent-localized vibrations may be considered separately. Varsányi[2] attempted to make a correspondence between the benzene vibrations and those of substituted benzenes, but this seems not to have been done consistently (for example between heavy and light substituents), and a numbered mode of a substituted benzene may not resemble its correspondingly numbered benzene mode very closely; and so, as we have noted in the above and in Ref. 1 (and as have others, see citations in Ref. 1), the actual process does not seem to be viable.

Hickman *et al.*[3] have compiled a full, selected, set of assignments for the vibrational frequencies of toluene in the S_0 electronic state; this was based upon a survey of ten previous infrared and Raman studies.[2,4–13] In that work, mainly the Mulliken labelling scheme was employed, with the Wilson labels, as assigned by Varsányi,[2] also being given, along with assignments from previous authors. It was noted therein[3] that the Wilson nomenclature had limited use, and this has also been noted by Tusumi *et al.*,[11] who introduced a new, but rather complicated, nomenclature for the toluene vibrations.

Hickman *et al.*[3] also recorded a fluorescence excitation spectrum for toluene in a jet-cooled molecular beam, extending to ~2000 cm^{-1} internal energy for the S_1 state. Assuming C_{2v} symmetry, the electronic transition $S_1 \leftarrow S_0$ corresponds to the promotion of an electron from the highest occupied molecular orbital with b_1 symmetry, to the lowest unoccupied orbital of a_2 symmetry, and so the transition can also be written $\cdots(b_1)^1(a_2)^1\ \tilde{A}^1B_2 \leftarrow \cdots(b_1)^2(a_2)^0\ \tilde{X}^1A_1$. The majority of the observed absorption features were identified with the aid of dispersed fluorescence, making use of the known S_0 frequencies to support these assignments, although it was noted that a few of those assignments were not wholly certain. These measurements yielded frequencies for 13 normal modes in the S_1 excited state, which were compared with the early UV absorption measurements of Ginsburg *et al.*,[14] which in turn were based on earlier experimental work by Savard[15] and Masaki[16] and theoretical work by Sponer,[17] with slightly later work by Kahane-Paillous and Leach.[18] There are also two-photon resonant spectra recorded via fluorescence by Vasudev and Brand[19] and via multiphoton ionization by Krogh-Jespersen *et al.*[20] Independent confirmation of some of the vibrational assignments were provided by Balfour and co-workers, who obtained infrared[21] and UV[22] absorption spectra for liquid toluene and seven deuterated isomers thereof. The S_1 state of toluene has also been studied in relation to complexes: Shauer *et al.*[23] report fluorescence spectra of toluene-He and toluene-CH_4 complexes; and Doyle *et al.*[24] report fluorescence spectra of toluene-rare gas complexes, while examining the heavy atom effect. Eisenhardt and Baumgärtel[25] reported the band origin energy of toluene from resonance-enhanced multiphoton ionization (REMPI) spectroscopy, but no REMPI spectra were actually shown therein.

The torsional motion of the methyl group has also been studied in detail. A combination of dispersed fluorescence and REMPI spectroscopy enabled Breen *et al.*[26] to derive an effective rotational constant for the methyl group, as well as the small energy barrier to its rotation in the S_0 and S_1 electronic states. Earlier work by Murakami *et al.*[27] also observed internal rotation in toluene via REMPI spectroscopy, but their assignments are not consistent with those of later work. Detailed consideration of the symmetry of the internal rotor levels, and consideration of the low-energy region of REMPI spectra of a number of toluene isotopologues, allowed Walker *et al.*[28] to gain understanding of which internal rotor bands appeared, as well as their intensities, by means of torsion-electronic coupling. (Recently, Kanamaru[29] presented a theoretical consideration of the vibronic interations in toluene, and concurred with these latter conclusions.) High resolution fluorescence excitation spectra have been reported by East *et al.*[30] for mono- and di-deuteration of the methyl group; and contemporaneously by Borst and Pratt.[31] These studies showed that the methyl group prefers a staggered conformation in both the S_1 and S_0 electronic states, where both non-deuterated toluene (designated Tol-h_8 herein) and α-trideuterated toluene, $C_6H_5CD_3$ (designated Tol-d_3 herein) were studied. Both of these high-resolution studies reported their spectra over narrow wavenumber regions of the origin, with the second also targeting an internal rotor level. We shall discuss the internal rotational structure further in the below.

Detailed studies on the toluene cation have been less extensive. Early photoionization work, yielding ionization energies, has been reported by Watanabe *et al.*[32,33] and photoelectron spectra were reported by Debies and Rabalais,[34] where some vibrational structure was seen. The ground cationic state has the electronic configuration $\cdots(b_1)^1$ and is designated $\tilde{X}^2B_1$, but we will frequently use D_0^+ in the below. The first report of the application of time-of-flight photoelectron spectroscopy to toluene appears to be that of Meek *et al.*[35] who employed a (1 + 1) ionization process in which the molecule was first promoted to a selected vibrational level within the S_1 manifold and then ionized by a second photon of the same energy; the kinetic energies of the electrons were then analyzed by time-of-flight. The authors were able to observe vibrational progressions in the photoelectron spectra taken *via* three different intermediate S_1 vibrational levels, but only tentative assignments were possible. Eisenhardt and Baumgärtel[25] used a similar technique to study toluene, observing vibrational structure, but the emphasis in that paper was on complexes. Shaw *et al.*[36] used synchrotron radiation as the direct photoionization source to obtain detailed information on a number of toluene cationic states via photoelectron spectroscopy. More recently, using a combination of time-of-flight and velocity map imaging techniques, Whiteside *et al.*[37] recorded photoelectron spectra *via* a series of S_1 vibrational levels and were able to assign seven cation frequencies. However, the vibrational features were only partially resolved, and the spectra recorded from intermediate levels >750 cm^{-1} above the S_1 origin were unstructured. This work was extended to picosecond studies of intramolecular vibrational redistribution (IVR) in both an accompanying paper[38] as well as a later paper,[39] which concentrated on a specific Fermi resonance[40] at 460 cm^{-1}. Improved spectra of the latter were reported recently in a time-resolved study, with a detailed analysis.[41]

Zero kinetic energy (ZEKE) photoelectron spectroscopy employing nanosecond lasers offers far greater resolution than the time-of-flight photoelectron method, and has enabled a detailed study of the torsional levels in the toluene cation by Lu *et al.*[42] Using the closely related mass analysed threshold ionization (MATI) technique, in which ions rather than electrons are detected following the ionization of Rydberg states by a pulsed electric field, Gunzer and Grotemeyer[43] were able to obtain well-resolved spectra from vibrational levels of the S_1 state of toluene.

In the present work, we use the ZEKE technique to explore the vibrations of the toluene cation in detail. These experiments are complementary to the time-resolved studies[38,39,41] but owing to the use of a nanosecond laser, which has a considerably narrower bandwidth (0.3 cm^{-1}), we are generally able to select single vibrational eigenstates within the intermediate S_1 electronic state cleanly; we shall discuss the time-resolved experiments in the light of our own experiments in the below. We shall also compare our ZEKE results to the dispersed fluorescence spectra of Hickman *et al.*,[3] gaining further insight into the assignment of the S_1 levels. Additionally, in an accompanying paper, Gascooke and Lawrance[44] present their results obtained from a detailed two-dimensional laser-induced fluorescence (2D-LIF) study of the Fermi resonance features at ∼460 cm^{-1}. As will be seen, there is excellent agreement between the two sets of results regarding those features, as well as with the results of the time-resolved photoelectron study.

II. EXPERIMENT

The apparatus employed has been described previously in detail in Ref. 45, incorporating small modifications in order to perform the ZEKE experiments, which have also been described,[46] and so only a brief description is given here. The second (532 nm) and third (355 nm) harmonics of a neodymium-doped yttrium aluminium garnet laser (Nd:YAG, Surelite III, 10 Hz) were each used to pump one of two tuneable dye lasers (Sirah Cobra Stretch). The pump dye laser was operated on Coumarin 503, while Pyrromethene 597 was used in the probe laser. The fundamental frequencies produced by each dye laser were frequency doubled using BBO and KDP crystals for the pump and probe lasers, respectively.

Tol-h_8 (Acros, 99.5% purity) or Tol-d_3 (Aldrich, 99 atom% D) vapour was seeded in ∼2 bars of Ar and the gaseous mixture passed through a General Valve pulsed nozzle (750 μm, 10 Hz, opening time of 210 μs) to create a free jet expansion. The focused, frequency-doubled output of both dye lasers were overlapped spatially and temporally and passed through a vacuum chamber coaxially and counterpropagating. Here they intersected the free jet expansion between two biased electrical grids located in the extraction region of a time-of-flight mass spectrometer.

(1 + 1) REMPI spectroscopy was utilized in order to determine the pump frequencies required to prepare each vibrational level in the S_1 state of toluene selectively. The intensities of the two overlapped laser beams were then adjusted to obtain a large enhancement of the ion signal owing to the two-colour, (1 + 1′) process. The voltages on the lens assembly were changed for the pulsed-field ionization, zero-electron-kinetic energy (PFI-ZEKE) photoelectron spectroscopy. The upper lens element was terminated to ground, whilst a fast rising pulsed positive potential was applied to the lower plate, both to pulse-field ionize high-lying Rydberg states and to extract the resulting ZEKE electrons. For the present experiments, it was found that a field of 5 V cm^{-1} resulted in the most intense ZEKE signals. The electrons were detected via a second dual microchannel plate detector, which was located ∼2 cm below the electrical extraction grids.

In the present experiments, it was confirmed that the photoionization cross-section for toluene was about an order of magnitude lower than that of the *para*-fluorotoluene (pFT) molecule we have studied previously;[47] this is in line with conclusions reached by Bacon and Hollas[48] with regard to the oscillator strength of the $S_1 \leftarrow S_0$ transition for toluene compared to other monosubstituted benzenes. As such, there was a continual compromise between resolution and signal-to-noise ratios in the ZEKE spectra and this limited the range of S_1 resonances we could employ as intermediates. In most cases in the present work, we estimate a typical ZEKE resolution of ∼8–10 cm^{-1}, and from approximate rotational simulations of the S_1 bands observed we estimate a typical rotational temperature of ∼5 K, although under the best conditions, rotational temperatures of ∼2 K were obtained.

The excitation laser has been calibrated by comparison of the bands observed in the (1 + 1) REMPI spectrum in the present work and the fluorescence excitation spectrum reported by Hickman *et al.*,[3] with the origin position calibrated to that reported by Borst and Pratt;[31] use was also made of the known positions of the S_1 origin of *p*FT,[47] observed in a recent series of experiments with an absolute error of ±1 cm^{-1}; we estimate our relative error to be ∼0.5 cm^{-1}. Calibration of the ionization laser has been performed through comparison of the ZEKE bands observed in the present work and those seen for toluene by Lu *et al.*[42]

III. COMPUTATIONAL METHODOLOGY

As an aid to the assignment of our spectra, the vibrational frequencies of toluene were calculated using the GAUSSIAN 09 software package,[49] where all of the calculations used default parameters. For the S_0 ($\tilde{X}^1A_1$) state, B3LYP/aug-cc-pVTZ calculations were employed; for the S_1 ($\tilde{A}^1B_2$) state TD-B3LYP/aug-cc-pVTZ calculations; and for the ground state cation ($\tilde{X}^2B_1$) state, UB3LYP/aug-cc-pVTZ, which yielded $\langle S^2 \rangle$ values of ∼0.76, indicating spin contamination was minimal.

The geometry of each electronic state was optimized and it was confirmed that the methyl group had to be oriented in a "staggered" conformation for the S_0 and S_1 states, with one of the C–H bonds perpendicular to the benzene ring, in order to obtain all real vibrational frequencies, in agreement with the earlier deductions from a fluorescence excitation study by Borst and Pratt.[31] In contrast, for the ground state cation, it was found that the eclipsed conformer was a minimum, in agreement with the finding of Weisshaar and co-workers.[28,42]

For the S_0 and D_0^+ electronic states, both harmonic and anharmonic frequencies were obtained for each of Tol-h_8 and

TABLE I. Calculated and experimental wavenumbers for the S_0 state of Tol-h_8 and Tol-d_3.

				Harmonic frequencies		Anharmonic frequencies		Experiment	
$\mathscr{M}_i$	HGL	Varsányi	Duschinsky mixing	h_8	d_3	h_8	d_3	h_8(HGL)[a]	d_3 (BF)[b]
				a_1					
1	1	20*a*	2 (13,7a)	3189	3189	3045	3045	3087	3087
2	2	2	20a,7a (13,2)	3168	3168	3036	3037	3063	3063
3	3	7*a*	13,7a (13)	3154	3154	2999	2990	3055	3056
4	5	9*a*	9a	1645	1645	1604	1606	1605	1606
5	6	18a	18a	1532	1532	1499	1500	1494	1495
6	8	13	(1,7a,20a,12,19a,13,2)	1230	1249	1202	1218	1210	1225
7	9	8a	8a	1204	1204	1191	1195	1175	1181
8	10	19a	19a (12,1)	1053	1049	1035	1033	1030	1026
9	11	12	12,1	1022	1022	1008	1008	1003	1003
10	12	1	1,6a (12,20a,7a,19a,13,2)	800	773	786	761	785	758
11	13	6a	6a (20a,7a)	529	506	525	501	521	498
				a_2					
12	14	17a	17a	994	995	976	982	964	966
13	15	10a	10a	863	862	848	848	843	845
14	16	16a	16a	417	417	409	411	407	406
				b_1					
15	20	5	5,17b	1013	1014	995	996	978	980
16	21	17b	17b,10b (5)	921	865	902	842	895	930
17	22	11	10b,11 (4)	750	726	740	710	728	709
18	23	4	4,11	717	704	705	694	695	687
19	24	16b	16b,11 (10b)	478	460	474	452	464	446
20	25	10b	16b (10b,11,17b,5)	210	195	210	197	216	206
				b_2					
21	26	7b	20b,7b	3176	3176	3033	3017	3039	3038
22	27	20b	7b,20b	3155	3155	3016	3021	3029	3029
23	29	9b	9b	1624	1620	1584	1584	1586	1586
24	31	18b	18b (3)	1472	1482	1441	1454	1445	1448
25	32	3	15,3	1362	1360	1343	1331	1330	...
26	33	8b	15,3 (8b)	1327	1321	1286	1307	1280	1300
27	34	14	14,8b	1181	1181	1168	1169	1155	1154
28	35	19b	19b (8b,14)	1112	1104	1092	1084	1080	1073
29	37	6b	6b	638	637	633	631	623	623
30	38	15	8b,19b (14,6b,3,18b)	343	306	364	310	342	307
				Methyl-localized					
	17	ν_{as}	...	3100	2297	2940	2214	2979	2230
	28	ν_{as}	...	3073	2272	2928	2191	2952	2209
	4	ν_s	...	3022	2174	2908	2096	2921	2130
	30	δ_{as}^+	...	1504	1073	1486	1071	1463	1050
	18	δ_{as}^+	...	1490	1069	1476	1064	1450	1050
	7	δ_s	...	1415	1078	1405	1079	1379	1040
	19	δ_{as}^-	...	1067	955	1044	936	1040	...
	36	δ_{as}^-	...	1002	804	998	788	967	...

[a]Reference 3.
[b]Reference 21.

Tol-d_3. As noted above, we label the S_0 vibrational modes by comparing the molecular vibrations with those of fluorobenzene, as discussed in our previous paper;[1] this gives a clear and unambiguous assignment of the vibrational modes which are ring-localized. The CH_3-localized vibrations are easily identified and standard symbols have been given in Table I to identify these (with the assignment coming from a combination of previous work and visualization). For the S_1 state, it was not possible to calculate the anharmonic frequencies, owing to technical restrictions in the program employed. For both the S_1 and D_0^+ states, the vibrational motions were sometimes altered somewhat from the S_0 motion, but it was always possible to identify the most appropriate $\mathscr{M}_i$ label in each case. Such assignments will, however, not include any strong resonance effects, such as Fermi resonance; in such cases, the actual eigenfunctions will correspond to mixtures of the $\mathscr{M}_i$ motions. The calculated values are presented in Tables II and III for the S_1 and D_0^+ states, respectively.

TABLE II. Calculated harmonic wavenumbers for the S_1 state of Tol-h_8 and Tol-d_3.

$\mathscr{M}_i$	HGL	Varsányi	Toluene-h_8	Toluene-d_3
		a_1		
1	1	20a	3213	3213
2	2	2	3191	3191
3	3	7a	3183	3182
4	5	9a	1578	1578
5	6	18a	1458	1459
6	8	13	1221	1247
7	9	8a	1177	1178
8	10	19a	974	973
9	11	12	990	992
10	12	1	768	740
11	13	6a	466	449
		a_2		
12	14	17a	719	719
13	15	10a	579	579
14	16	16a	217	217
		b_1		
15	20	5	822	831
16	21	17b	716	696
17	22	11	599	594
18	23	4	450	430
19	24	16b	322	318
20	25	10b	150	142
		b_2		
21	26	7b	3204	3204
22	27	20b	3185	3185
23	29	9b	1539	1534
24	31	18b	1470	1421
25	32	3	1415	1327
26	33	8b	1175	1175
27	34	14	1441	1450
28	35	19b	1059	1026
29	37	6b	538	536
30	38	15	339	302
		Methyl-localized		
	17	ν_{as}	3079	2281
	28	ν_{as}	3029	2126
	4	ν_s	2936	2219
	30	δ_{as}^+	1471	1062
	18	δ_{as}^+	1387	1042
	7	δ_s	1331	1037
	19	δ_{as}^-	997	821
	36	δ_{as}^-	956	789

TABLE III. Calculated wavenumbers for the D_0^+ state of Tol-h_8 and Tol-d_3.

			Toluene-h_8		Toluene-d_3	
$\mathscr{M}_i$	HGL	Varsányi	Harmonic	Anharmonic	Harmonic	Anharmonic
			a_1			
1	1	20a	3213	3076	3213	3076
2	2	2	3199	3069	3199	3077
3	3	7a	3190	3069	3190	3060
4	5	9a	1672	1576	1672	1568
5	6	18a	1474	1431	1476	1444
6	8	13	1258	1227	1278	1253
7	9	8a	1218	1186	1222	1189
8	10	19a	988	984	981	967
9	11	12	1009	982	1004	983
10	12	1	776	762	749	740
11	13	6a	520	508	491	476
			a_2			
12	14	17a	1027	1010	1024	1006
13	15	10a	808	774	807	770
14	16	16a	351	348	351	351
			b_1			
15	20	5	1039	1049	1039	1044
16	21	17b	947	930	981	969
17	22	11	754	736	702	683
18	23	4	581	583	536	541
19	24	16b	386	388	377	379
20	25	10b	152	154	143	146
			b_2			
21	26	7b	3210	3046	3210	3100
22	27	20b	3194	3065	3194	3065
23	29	9b	1406	1380	1406	1373
24	31	18b	1538	1499	1538	1499
25	32	3	1394	1352	1392	1355
26	33	8b	1297	1264	1298	1265
27	34	14	1165	1147	1155	1133
28	35	19b	1085	1069	1085	1072
29	37	6b	500	493	507	500
30	38	15	346	330	308	297
			Methyl-localized			
	17	ν_{as}	3150	2978	2332	2232
	28	ν_{as}	3006	2874	2215	2143
	4	ν_s	2981	2864	2148	2067
	30	δ_{as}^+	1427	1371	1033	1009
	18	δ_{as}^+	1483	1456	1071	1045
	7	δ_s	1359	1316	994	975
	19	δ_{as}^-	1009	985	879	871
	36	δ_{as}^-	973	965	801	784

IV. RESULTS AND ASSIGNMENT

A. The vibrations of the S_0 electronic state

1. Background

Since a large factor in the assignment of the vibrations of the S_1 state is by comparison with observed activity in dispersed fluorescence; and since, in turn, the assignments of the D_0^+ vibrations depend on those in the S_1 state, it is important to be sure that the S_0 assignments are sound. As we highlighted in Ref. 1, there have been a number of inconsistencies in applying the Wilson labels to some of the vibrational modes in benzene, which has been propagated into work on substituted benzenes. We do not reproduce the details here, but note that some or all of the following switches in Wilson mode numbering for benzene are often required in order to assign the correct wavenumber to the correct vibrational motion: 8a ↔ 9a, 8b ↔ 9b, 18a ↔ 19a, 18b ↔ 19b, and 3 ↔ 14.

As noted above, Hickman *et al.*[3] undertook a detailed review of the previous assignments of the vibrations of the ground electronic state of toluene. As may be seen from Table I of that work, there have been significant disagreements regarding the assignment of the observed frequencies.

Hickman *et al.*[3] selected frequencies for each of the vibrations, identified by a set of Mulliken labels, noting that the evidence for some of the choices was not strong. In a comment at the end of that paper, the authors of Ref. 3 noted the study by Balfour and Fried,[21] which led them to suggest some minor modifications to these assignments.

In Table I of the present work, we give the harmonic and anharmonic calculated vibrational frequencies of toluene determined from B3LYP/aug-cc-pVTZ calculations. We also include a column which indicates how each vibration in toluene corresponds to those in benzene, as calculated using the Duschinsky matrix approach, and employing the "artificial isotope" calculations using the fluorobenzene force field; that is, we identify the ring-localized vibrations of toluene with those of fluorobenzene containing the artificial ^{15}F isotope. (This approach is discussed in more detail in Ref. 1.) We employ the FC-LabII program,[50] written by and recently employed by Pugliesi *et al.*[51] in their similar analysis of the fluorobenzene vibrations. In our entries in Table I, if the normalized mixing coefficient for a benzene contribution is greater than 0.2, it is listed as a major contribution with no parentheses; if the contribution is between 0.05 and 0.2, then this is counted as a minor contribution and listed inside parentheses; if there is more than one major and/or minor contribution, then these are listed in descending importance; contributions < 0.05 are ignored; finally, we call a contribution with a mixing coefficient > 0.5 a majority contribution.

As may be immediately seen, and in line with both our previous deductions[1] and those of Pugliesi *et al.* with regards to fluorobenzene,[51] many of the modes cannot be described in terms of a simple benzene Wilson label, and a number are highly mixed, having no majority contribution in many cases. Thus, the use of the Wilson nomenclature is of very little help, and indeed is very misleading for conveying the actual atomic motions for the vibrations of toluene. The $\mathscr{M}_i$ labelling we give corresponds to the mode diagrams given in Ref. 1: these are much more indicative of the actual motion of the atoms in toluene, under the assumption that the methyl group may be treated as a point mass. As a consequence of their construction, the $\mathscr{M}_i$ labels are the same for toluene (both isotopologues), as well as fluorobenzene and chlorobenzene, and we shall make use of this when we compare activity in the electronic and ZEKE spectra later on.

For toluene, symmetry labels are somewhat problematic. The presence of the methyl group strictly reduces the symmetry to C_s, assuming it is oriented in either the staggered or eclipsed conformations; although the z axis is oriented differently in each of those cases. When discussing vibrations and electronic states of monosubstituted benzenes, it is common to employ the C_{2v} point group: i.e., under the approximation that the substituent is a point mass, whether it is an atom or not. Together with our method of assigning the $\mathscr{M}_i$ labels, we can then assign *pseudo*-C_{2v} symmetry labels to the ring-localized modes, and we give these in Table I for the ring-localized modes. It is well known that the $S_1 \leftarrow S_0$ ($\tilde{A}^1B_{2u} \leftarrow \tilde{X}^1A_{1g}$) transition for benzene is formally forbidden, but becomes allowed because of Herzberg-Teller coupling to the optically allowed $\tilde{C}^1E_{1u}$ state; this coupling may be seen from activity in e_{2g} vibrational modes in the $S_1 \leftarrow S_0$ spectrum. In the monosubstituted halobenzenes, the symmetry is now C_{2v} and so formally this transition becomes allowed, and this is seen from the increased oscillator strength of this transition when compared to that of benzene.[52] However, as is often stated, the electronic structure still has a memory of the D_{6h} symmetry and the vibronic nature of the transition; alternatively, even though the geometry is formally not D_{6h}, the electronic structure of the ring is largely unchanged from benzene.[52] As a consequence, we would expect the toluene vibrations which correspond to the e_{2g} vibrations of benzene to be active; these are the $\nu_{6a/b}$, the $\nu_{7a/b}$, the $\nu_{8a/b}$, and the $\nu_{9a/b}$ vibrations. Although the equivalent a_1 components of these vibrations are formally allowed under C_{2v} symmetry, it is interesting to note that they, as well as the b_2 components, are often seen strongly in spectra of monosubstituted benzenes; we note, in particular, the ν_{6a} (largely $\mathscr{M}_{11}$ here) and the ν_{6b} (largely $\mathscr{M}_{29}$ here) vibrations in the low wavenumber region of the $S_1 \leftarrow S_0$ spectrum of monosubstituted benzenes; it is interesting to note that although the $\mathscr{M}_{29}$ vibration always appears strongly in $S_1 \leftarrow S_0$ transitions, the $\mathscr{M}_{11}$ vibration can sometimes be quite weak, suggesting it is sensitive to the nature of the substituent (not just its mass).

As discussed in the above, there is some confusion in the literature regarding the labelling of the vibrations of toluene in terms of C_{2v} symmetry labels and the subsequent numbering of these according to the Mulliken scheme. Hickman *et al.*[3] note the confusion in the literature surrounding the Wilson labelling of the vibrations, and sought to clarify the issue by using Mulliken numbering. In doing this, as well as assigning C_{2v} labels to the ring-localized vibrations, under the assumption that CH_3 is a point mass, they also do the same for the CH_3-localized vibrations. However, it is not possible to determine how these vibrations transform under the C_{2v} point group symmetry operations, as not all symmetry elements are present; in short, we are unsure how these C_{2v} labels were arrived at, and this therefore transfers also onto the Mulliken numbering. We feel this is further ammunition for employing our labelling scheme, where the ring-localized vibrations are separated from the methyl-localized ones, for toluene.

2. Assignment

We now return to the specific assignments of the vibrations of the S_0 state. As noted in the above, Hickman *et al.*[3] have selected a set of vibrational frequencies for Tol-h_8, and numbered them, ostensibly according to the Mulliken scheme (but see comments in Subsection IV A 1), and these are listed in Table I, where we give their Mulliken labels, as well as our $\mathscr{M}_i$ labels; additionally we provide the Varsányi versions of the Wilson labels, which we emphasise are not always indicative of the actual atomic motions. The $\mathscr{M}_i$ labels allow the vibrational motion to be deduced from the mode diagrams for the ring-localized vibrations (see Ref. 1); the methyl vibrations are identified with the labels given by Varsányi[2] and confirmed by the calculated vibrational motions. The Tol-d_3 values are taken from Balfour and Fried,[21] where the values presented therein were largely based on those of Lau and

Snyder[7] and Morrison and Laposa.[13] We have taken note of various discrepancies between the ordering of the values in Refs. 3 and 21 for Tol-h_8, and so here we have mainly used the values presented in Table 1 of Ref. 21, using the Tol-d_3 value that corresponds most closely to the recommended Tol-h_8 value in Ref. 3. After doing this, it becomes clear that the vast majority of the values are consistent with the calculated values, including the isotopic shifts. There are a few cases, however, where the assignment needs to be considered in some detail, and these instances are discussed in the below.

Overall, we see from Table I that, for the most part, our calculated anharmonic frequencies for both Tol-h_8 and Tol-d_3 are generally in very good agreement with the experimental values. Hickman *et al.*[3] noted that the assignments of the higher wavenumber modes (>3000 cm^{-1}) for Tol-h_8 have been rather erratic, with the actual Wilson label given changing frequently between publications. It is clear from the Duschinsky mixing (see the fourth column of Table I) that these high frequency modes cannot be regarded as any individual Wilson mode, perhaps with the exception of the $\mathscr{M}_1$ mode, which has a majority contribution from Wilson mode 2. We note that the trend in these high-wavenumber vibrations having a calculated anharmonic wavenumber slightly lower than the experimental one suggests that the frequencies given in Varsányi's book for $\mathscr{M}_1$, $\mathscr{M}_2$ and $\mathscr{M}_3$ are in best agreement with our values. The few Tol-h_8 modes which are between 2900 and 3000 cm^{-1} are straightforwardly assigned to methyl-localized vibrations, with the corresponding Tol-d_3 ones also being consistent. The a_2 modes are all very well described by Wilson modes, and this seems to be generally true,[1] and their assignment seems clear for both Tol-h_8 and Tol-d_3, given the consistency of agreement with previous work. With regard to the b_1 modes, these have mixed-Wilson character and so are best described by the $\mathscr{M}_i$ labels given, notwithstanding a number of consistent assignments in previous work. With regard to the b_2 vibrations with a wavenumber <1600 cm^{-1}, we note that $\mathscr{M}_{23}$ may be identified with the Wilson mode 9*b* (note the comments in the above with regard to the switch in labelling of the Wilson modes of benzene—these changes have already been made in Table I), and that $\mathscr{M}_{29}$ can be identified as the Wilson mode 6*b*. All other vibrations have mixed Wilson mode character, and so use of such labels is not advised; the $\mathscr{M}_i$ labels more clearly identify the atomic motions. Some discussion was presented in Ref. 3 regarding Tol-h_8 bands in the range 1450–1465 cm^{-1}, which had different values and/or assignments in earlier work; it was decided that the ring-localized vibration ($\mathscr{M}_{24}$ here) of b_2 symmetry was likely to be at 1445 cm^{-1}, with a second designated b_2 vibration (see comments above regarding the inappropriateness of assigning C_{2v} symmetry labels to the methyl vibrations) at 1463 cm^{-1} being a methyl-localized band. (There is another methyl-localized band observed at 1450 cm^{-1}.) These assignments are in line with our calculated vibrational wavenumbers, which also suggest the methyl-localized vibrations will have higher values than the ring-localized vibration. The corresponding Tol-d_3 $\mathscr{M}_{24}$ value is in equally good agreement with the calculated value, showing a very small positive shift upon deuteration. For the methyl-localized vibrations, however, very significant shifts to low wavenumber are calculated. The experimental values in Ref. 21 are given the same value for both Tol-h_8 and Tol-d_3; in Table I we have employed the different Tol-h_8 values from Ref. 3, but give the same experimental wavenumber values from Ref. 21 for Tol-d_3.

We now move onto the three vibrational features observed at 1330, 1312, and 1280 cm^{-1} for Tol-h_8 in gas phase studies, which were considered in Ref. 3. The first was not given an explicit assignment, the second was assigned as Wilson mode 14, which we have noted should really be designated Wilson mode 3 ($\mathscr{M}_{25}$ here); and the last as Wilson mode 3, which we have noted should really be designated Wilson mode 14 ($\mathscr{M}_{27}$ here). We have some issues with these assignments, which are not consistent with the cited values by Balfour and Fried.[21] Our calculations suggest that the 1280 cm^{-1} value is more likely to be $\mathscr{M}_{26}$, while the value of 1330 cm^{-1} seems to agree better with the anharmonic calculated wavenumber for $\mathscr{M}_{25}$ than does the 1312 cm^{-1} value. It is not clear what the latter wavenumber corresponds to, although a combination band $\mathscr{M}_{29}\mathscr{M}_{30}^2$ might be possible, as is the combination $\mathscr{M}_{10}\mathscr{M}_{11}$. We note that Hickman *et al.*[3] assigned a dispersed fluorescence band observed at 1317 cm^{-1} to $\mathscr{M}_{11}\mathscr{M}_{14}^2$, which would imply anharmonic effects; however, a band at 1317 cm^{-1} was also observed in a phosphorescence study,[53] with a possible assignment to $\mathscr{M}_{25}$ offered. We have noted that we prefer a different value for $\mathscr{M}_{25}$; the other offered assignment was to a combination band. The difficulty of assigning these features may arise from a number of possible fundamentals and combinations with wavenumbers in this region, thus there is the possibility of Fermi resonance shifts. Hence the current assignments for Tol-h_8 given in Table I of the present work must still be taken as a best attempt. If we compare to the Tol-d_3 values from Ref. 21, then things are equally unclear. Two bands are given in this range, at 1261 cm^{-1} and 1300 cm^{-1}, assigned to Wilson modes 3 and 14 (as stated in Ref. 21—see comments above regarding the numbering of these modes). The calculations suggest that the $\mathscr{M}_{25}$ vibration will have a small isotopic shift to lower wavenumber upon deuteration, with a slightly larger positive shift for $\mathscr{M}_{26}$. Looking at the calculated values, it would seem more likely that the 1300 cm^{-1} band is $\mathscr{M}_{26}$, with the assignment of the 1261 cm^{-1} vibration uncertain. We note that the phosphorescent study[53] suggests a value of 1316 cm^{-1} as a fundamental for Tol-h_8, which would be in very good agreement with our calculated value for the $\mathscr{M}_{25}$ mode; this value was, however, recorded in a benzene matrix at 4 K, and so could be shifted from the gas phase value.

We note that a band at 967 cm^{-1} band was commented on in Ref. 3 and assigned to Mulliken mode 36 for Tol-h_8 in their tables (a methyl-localized vibration), but the wavenumber for this mode was altered in the Note Added in Proof to a value of 1040 cm^{-1} based upon the work of Balfour and Fried.[21] Both of these assignments are in fair agreement with the anharmonic calculated wavenumber of 965 cm^{-1}. However, a possible assignment for the 1040 cm^{-1} vibration is the overtone $\mathscr{M}_{11}^2$ and a possible assignment of the 967 cm^{-1} vibration is to the $\mathscr{M}_{29}\mathscr{M}_{30}$ combination band. Clearly the definitive assignment of these features is still troublesome.

B. REMPI and ZEKE spectra of Tol-h_8 and Tol-d_3

1. General remarks

When assigning the vibrations of excited electronic states of monosubstituted benzenes, it is conventional to use the same vibrational labels as the ground state. Assignments based on experimental results make use of similarity to ground state frequencies in may cases, but where frequencies differ, assignment can be somewhat difficult and sometimes must be made with the benefit of rotational band profiles and (at least perceived) chemical insight. Calculations can clearly help in this regard, if they are deemed reliable. In the present work we are concerned with the lowest $\pi^* \leftarrow \pi$ excitation, which leads to the transition between electronic states represented by $S_1 \leftarrow S_0$ or, more explicitly, as $\tilde{A}^1B_2 \leftarrow \tilde{X}^1A_1$, assuming C_{2v} symmetry. In recent years, in tackling the assignment of such spectra, it has become commonplace to calculate vibrational frequencies for the S_1 state to compare with experiment, using a variety of approaches. Recent work by Pugliesi *et al.*[51] on fluorobenzene has shown that although reasonable agreement can be obtained with different methods, even with highly sophisticated methods obtaining good agreement with experiment for the excited singlet state is still challenging. In part this is due to neglect of anharmonicity (including possible couplings between vibrations) and vibronic effects; but there are often issues arising from the effects of dynamic and non-dynamic correlation—both of these effects are difficult to explore in detail, owing to the size of the systems and so cost of the calculations.

To assign electronic spectra, much use is made of the "$\Delta v = 0$" propensity rule which states that, assuming that the geometric structure does not change too much during an electronic transition, then the Franck-Condon factors between the states will be close to diagonal. As a consequence, whichever vibration was excited in one state, will be excited after the electronic transition. A significant Duschinsky rotation would mean that there will not necessarily be a direct correspondence between vibrations assigned in the S_0 state, with those in the S_1 state, and so a vibration in one state could be a linear combination of more than one in the other state; hence, after the electronic transition, more than one vibration could be excited—an effect called Duschinsky mixing or Duschinsky rotation. This means that some vibrations in the S_1 state, for example, are better described as linear combinations of the S_0 ones. The authors of Ref. 3 have identified a number of such instances of this; however, in the region examined in the present work, these effects appear to be minimal and the ground state labels can safely be applied. Indeed, the $\Delta v = 0$ propensity rule has proven to be a powerful tool in assigning such spectra, as long as it is borne in mind that is only an approximation, albeit a good one. In the present case, for the $S_1 \leftarrow S_0$ transition, we expect to be exciting from the zero-point vibrational level almost exclusively; in the ZEKE spectra, however, we shall be selecting various S_1 vibrational levels and so will make use of the $\Delta v = 0$ rule when assigning these spectra.

We now move onto a discussion of the REMPI spectra. For Tol-h_8 we shall compare to the LIF and DF results of Hickman *et al.*[3] For both Tol-h_8 and Tol-d_3 we shall also refer to the ZEKE spectra, to confirm and/or aid in the assignment. To aid the discussion, we shall consider the features in the REMPI spectrum over sets of wavenumber ranges, discussing the assignment and presenting the ZEKE spectra as we go. Additionally, we shall compare to corresponding spectra for fluorobenzene and chlorobenzene. We anticipate that, at least for the monosubstituted species, the assignments of the observed features should be largely consistent. Further, the observed spectra should be consistent between Tol-h_8 and Tol-d_3.

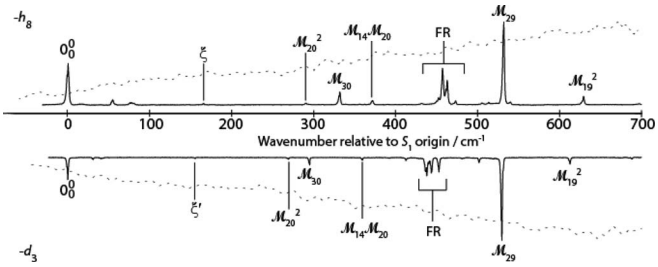

FIG. 1. (1 + 1) REMPI spectra of Tol-h_8 (upright) and Tol-d_3 (inverted) in the range 0–700 cm^{-1}. The assignment of the bands marked as ξ and ξ_i are discussed in the text. The features marked "FR" are Fermi resonances and are discussed in detail in the text. The dotted lines indicate the intensity of the uv light across the region. Expanded views of regions of these spectra are shown in Figures 2–5.

The 0–700 cm^{-1} ranges of the REMPI spectra for Tol-h_8 and Tol-d_3 are shown in Figure 1; expanded views of regions of the spectra are presented in later figures, together with a rationale of the assignments. The S_1 electronic state of Tol-h_8 has been the focus of a number of studies in the past as described above. The vibrational structure observed here compares well to the early jet-cooled fluorescence excitation spectrum of Hopkins *et al.*,[54] and also to the later spectra reported by both Hickman *et al.*,[3] and Doyle *et al.*[24] Good agreement is also seen with the (1 + 1) REMPI spectrum recently reported by Davies *et al.*[41] and the (1 + 1) REMPI spectrum recorded by Gunzer and Grotemeyer.[43] It is noted that the relative intensities of several bands observed in the (1 + 1) REMPI spectrum reported in the present work differ from those observed in previous studies, particularly the origin band; this is attributed to the varying UV intensity across the wavenumber range of this spectrum. In order to allow the reader to gauge this, the UV intensity, as recorded using a photodiode, is plotted along with the (1 + 1) REMPI spectrum; we note that this is only indicative as the response (including offset) of the photodiode is uncertain, and we thus refrain from attempting to normalize the spectrum against this. As far as we are aware, this is the first time that the REMPI spectrum of Tol-d_3 has been presented over this range, although a small region showing the internal rotor bands (see below) was reported in Ref. 28.

The majority of the features in the Tol-h_8 spectrum have been assigned by earlier workers to vibrations of a_1 symmetry (C_{2v} symmetry implicitly assumed), as expected; however, as in similar work investigating other substituted benzene molecules, vibrations with b_2 symmetry are observed and have been attributed to vibronic interactions, as discussed

above. Owing to the improved resolution of the present study, in comparison to that of the previous picosecond study,[41] and improved signal-to-noise when compared to the fluorescence excitation spectrum of Hickman *et al.*,[3] we have been able to resolve several previously unreported features and the assignment of these will be discussed. Assignments of the Tol-d_3 spectrum will be made concurrently with those of Tol-h_8, since consistency between the two is generally expected. We also note that previous assignments of the vibrations observed in the S_1 spectra were, to a large extent, dependent on the assignment of the vibrations of the S_0 state, via the activity observed in dispersed fluorescence. The assignment of the S_1 vibrations in terms of a set of Mulliken labels has been discussed in some detail by Hickman *et al.*,[3] and in many cases we concur with their assignments. We shall now discuss the assignments of the Tol-h_8 and Tol-d_3 spectra simultaneously, separating the discussion to different wavenumber ranges. Concurrently, we shall discuss the ZEKE spectra of the two isotopologues in the cases when we recorded these, as these either confirm or help to determine the assignment.

2. 0–200 cm^{-1} region

This wavenumber region of the (1 + 1) REMPI spectra is shown in the upper trace of Figure 2 for both Tol-h_8 and Tol-d_3. There is a relatively intense origin band in each case, followed by a series of weak features. The origins peak positions are at 37476.8 cm^{-1} and 37501.7 cm^{-1} for Tol-h_8 and Tol-d_3, respectively; the former value was calibrated to that of Borst and Pratt,[31] while the latter is in good agreement with the value of 37504 cm^{-1} obtained by Balfour and Ram.[22] We note that Walker *et al.* reported the low-wavenumber region of the Tol-d_3 REMPI spectrum in Ref. 28, but only report the spectrum in relative wavenumbers; the appearance of the spectrum is similar to our own, however. It is interesting to note that the $S_1 \leftarrow S_0$ transition wavenumber is higher for Tol-d_3 than for Tol-h_8: this arises owing to greater overall shifts in zero-point vibrational wavenumber in the S_0 state compared to the S_1 state.

The weak features to higher wavenumber, but below 100 cm^{-1}, have been previously assigned to internal rotation of the methyl group.[26,28,30,31] The model adopted is a fixed phenyl ring, with the methyl group having an

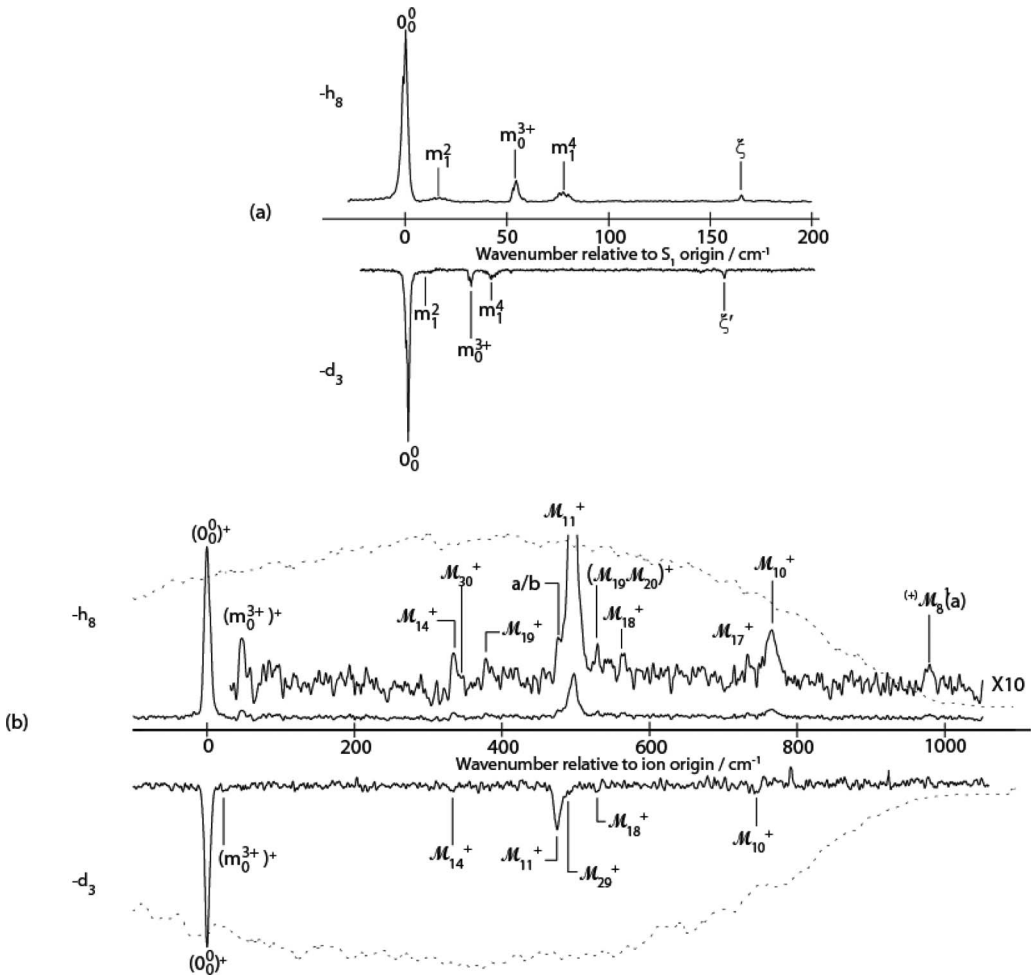

FIG. 2. (a) Expanded view of (1 + 1) REMPI spectra of Tol-h_8 (upright) and Tol-d_3 (inverted) in the range 0–200 cm^{-1}. The two bands marked with ξ and ξ_i are difficult to assign unambiguously, and are discussed in the text. (b) ZEKE spectra of Tol-h_8 (upright) and Tol-d_3 (inverted) via S_1 0^0; the Tol-h_8 ZEKE spectrum also shows an expanded version of the trace to allow the weaker, but reproducible, features to be seen. The dotted lines indicate the intensity of the uv light across the region.

effective rotational constant for internal rotation, B_{int}. Solution of the Schrödinger equation yields a set of internal rotor levels, with energies $B_{int}m^2$, where m is the internal rotation quantum number. The barrier to rotation, for a molecule such as toluene, creates a sixfold periodic potential with the barrier height represented by V_6. The effect of the barrier is to cause splitting of the pairs of degenerate levels, with this splitting being marked for levels with $m = 3$ but quite small for other levels, particularly when V_6 is small, as it is in toluene. The splitting of the $m = 3$ levels is approximately symmetric, with levels separated by approximately $|V_6/2|$;[55] the split levels are denoted $m = +3$ and $m = -3$, with their ordering dependent on the sign of V_6. The sign of V_6 is defined as being negative if the lowest energy structure is staggered (one of the methyl CH bonds perpendicular to plane of phenyl ring), and positive if the lowest energy structure is eclipsed (one of the methyl CH bonds in the same plane as the phenyl ring); for $V_6 < 0$, the $m = +3$ level would lie above the $m = -3$ one (and vice versa).

Which transitions are observed depends on symmetry, with the allowed transitions having been discussed in previous work;[26] the symmetry considerations relate to the G_{12} molecular symmetry group (which is isomorphic to the D_{3h} point group)—see Refs. 26 and 28 for further details. Consideration of the energies of the internal rotor states, and the observed bands, leads to the conclusion that the band at 54.9 cm^{-1} in Tol-h_8 must arise from one of the $m = 3$ bands, but whether it is the +3 or −3 level was initially not clear since transitions to both of these levels are symmetry-forbidden. Walker *et al.*[28] showed that torsional-electronic coupling with the nearby S_2 state ($\tilde{B}^1B_1$) could explain the observed bands, and that it further implied that it was the $m = +3$ level that was being accessed. In turn, this required that V_6 was negative and so the equilibrium geometry in the S_1 state was staggered, i.e., the same conformation as deduced from high-resolution fluorescence experiments,[31] where the derived (signed) value of V_6 in the S_0 state agreed with the $|V_6|$ value from microwave studies for the S_0 state.[56–58] Approximate B_{int} and V_6 parameters for the S_1 state have been reported in Refs. 26 and 28, but these have been refined by the high-resolution studies of Refs. 30 and 31. The values for both Tol-h_8 and Tol-d_3 are given in Table III, with the ground state values having been taken from the absolute values obtained in the microwave spectroscopic studies,[56–58] but with the sign coming from Borst and Pratt[31] and Walker *et al.*[28] The V_6 barriers are seen to be larger in the S_1 state than in the S_0 state. For the cation, we take the values for Tol-h_8 from Refs. 28 and 42, and estimate the values for Tol-d_3, based on the change in values between Tol-h_8 and Tol-d_3 in the other two states.

In Table IV are also presented the wavenumbers of the transitions between the internal rotor levels. As may be seen, "hot" bands are present, where the m quantum number in the lower state is not zero. In fact, these bands are not hot *per se* but arise from internal rotor levels with different overall nuclear spin symmetry (caused by the nuclear spins of the methyl H or D atoms): it is thus not possible for the $m = 1$ levels to be collisionally quenched efficiently into the $m = 0$ levels. In the present work, owing to the similarity in the B_{int} values, the $m' = 1 \leftarrow m'' = 1$ transition is unresolved from the $m' = 0 \leftarrow m'' = 0$ transition at the origin; the associated individual rotational lines have been resolved in Refs. 30 and 31. It is relatively straightforward to assign the $S_1 \leftarrow S_0$ bands at wavenumbers < 100 cm^{-1} for both Tol-h_8 and Tol-d_3 as shown in Figure 2, which match the assignments given in Ref. 28. The bands in Tol-d_3 are seen to lie at lower wavenumber than those for Tol-h_8, as expected, owing to its lower value of B_{int}, caused by the larger mass of D.

TABLE IV. Calculated positions of the internal rotor levels in Tol-h_8 and Tol-d_3 in the S_0, S_1, and D_0^+ states.[a]

		S_0 wavenumber		S_1 wavenumber		D_0^+ wavenumber	
m	Symmetry	Tol-h_8	Tol-d_3	Tol-h_8	Tol-d_3	Tol-h_8	Tol-d_3
0	a_1'	0	0	0	0	0	0
1	e''	5.4	2.8	5.3	2.7	5.3	2.7
2	e'	21.7	11.2	21.2	11.0	21.2	10.8
−3	a_2''	47.7	24.1	41.1	18.5	51.7	28.0
+3	a_1''	50.2	26.3	54.3	30.8	43.7	20.6
4	e'	87.0	44.8	84.8	43.8	84.8	43.2
5	e''	135.9	70.0	132.5	68.5	132.5	67.5
6	a_1'	195.7	100.8	190.7	98.6	190.8	97.2

[a]Wavenumber values calculated from $B_{int}m^2$, with the $m = +3$ and $m = -3$ values being additionally separated symmetrically from the $m = 3$ position, each by $V_6/4$. The B_{int} and V_6 values for the S_0 and S_1 state of Tol-h_8 were taken from Ref. 31; while those for Tol-d_3 were taken from Ref. 28. The values for the Tol-h_8 cation were taken from Ref. 42. The Tol-d_3 cation values were estimated as $B_{int} = 2.7$ cm^{-1} and $V_6 = +15$ cm^{-1} by comparing the Tol-h_8 cation values with the variations seen in the other states.

For the cation, internal rotor transitions were studied by Lu *et al.*,[42] and similar features for Tol-h_8 were seen in MATI spectra by Gunzer and Grotemeyer,[43] where agreement was noted with the Lu *et al.* spectra.

In the Tol-h_8 REMPI spectrum there is a weak band at 165.1 cm^{-1}, marked ξ, which appears to have a counterpart in the Tol-d_3 spectrum at 155.3 cm^{-1}, marked ξ'. Interestingly, the Tol-h_8 band has not been mentioned in recent work, although it can be seen in the fluorescence excitation spectrum of Doyle *et al.*,[24] recorded using helium as the backing gas. It is unfortunate that the signal-to-noise of the fluorescence excitation spectrum in Ref. 3 is not good enough to see this band. Balfour and Ram[22] have recorded absorption spectra of Tol-h_8 and Tol-d_3 vapour observing a wide range of fundamental, overtone, combination and hot bands. They only report a single band below 200 cm^{-1} for Tol-h_8, at 148 cm^{-1}, and none for Tol-d_3, and this band was assigned as a hot band therein. Perusal of the papers reporting earlier absorption spectra of Tol-h_8 reveals that Ginsburg *et al.*[14] observe a very weak band at 172 cm^{-1}, but this was unassigned. Krogh-Jesperson *et al.*[20] assign a band at 157 cm^{-1} above the origin to $\mathscr{M}_{20}$ in their two-photon REMPI spectra using visible light; they also observe the $\mathscr{M}_{20}$ 0–1 hot band at −224 cm^{-1}, and the $\mathscr{M}_{20}$ 1–1 sequence band at −61 cm^{-1}. There seems to be some inconsistency between the cited values, although the bands in Ref. 20 are quite broad as the spectra were recorded in a low-pressure static gas cell. In our view, this assignment is not definitive and it is not clear that we can assume that the 157 cm^{-1} feature observed in Ref. 20 is the same as our observed feature at 165.7 cm^{-1}.

As a consequence, the assignment of the 165.1 and 155.3 cm^{-1} bands for Tol-h_8 and Tol-d_3 turns out not to be so

straightforward. It is clear from calculating the energy levels for internal rotation (see Table IV) that there must be another source for these bands. In particular, the calculated wavenumber of the allowed $m' = 6 \leftarrow m'' = 0$ transition is significantly too high. The feature also cannot be attributed to toluene clusters, as these are very broad in appearance;[59] nor can it be due to toluene-argon complexes, as the same band is seen using helium as a backing gas.[24] In Table III the calculated vibrational wavenumbers for the S_1 state are presented and perusal of these shows that the only viable assignment of this band would be to the lowest-wavenumber b_1 mode, $\mathscr{M}_{20}$ (consistent with the Krogh-Jesperson *et al.*[20] paper). However, it becomes clear from the assignment of the other low-wavenumber features, that the $\mathscr{M}_{20}$ vibrational wavenumber in combination with other vibrations suggests a value somewhat lower than 165.1 cm^{-1} (see below). Intriguingly, there is a band at around 70 cm^{-1} in the REMPI spectrum of fluorobenzene,[51] which it is clear cannot arise from a cold vibrational band. As a consequence, it is possible that the assignments of both this, and the present 165.1 cm^{-1} feature, are to an as-yet-unidentified vibrational hot band. The lack of other hot bands in the present work would suggest differential cooling of the vibrational modes, some of which may become populated by cluster break-up during the supersonic expansion process. An alternative for Tol-h_8 is that indeed the 165.1 cm^{-1} feature is $\mathscr{M}_{20}$, but that there is significant anharmonicity for this vibration, whether in combination, or as an overtone. In retrospect, it is unfortunate we did not record a ZEKE spectrum via this feature, however this would have been challenging owing to its weak intensity. We comment further on this feature below.

In Figure 2 we also show the ZEKE spectra obtained via excitation through the origin for both Tol-h_8 and Tol-d_3. In the following, we will append a superscripted "+" to the vibrational and internal rotational labels to note these are for the cation; for overtones and combination bands, we will additionally employ parentheses for clarity. For Tol-h_8, the $m^+ = +3$ band is seen 48 cm^{-1} above the strong origin, which is calibrated to the 71199 cm^{-1} value reported by Lu *et al.*,[42,43] who also saw other internal rotational features; we did not attempt to improve our spectra in this region, as this was not the focus of our attention in the present work (this feature has also been observed by Whiteside *et al.*[37] and Gunzer and Grotemeyer[43]). Detailed consideration of the observed internal rotational features led Weisshaar and co-workers to conclude that the cation has an eclipsed geometry (one methyl C–H bond in the plane of the phenyl ring), with $V_6 > 0$.[28,42] For Tol-d_3, we measure the origin band at 71235 cm^{-1}, with the $m^+ = +3$ band being seen 22 cm^{-1} above the origin; this seems to be the first time this value has been reported. Similar to the origin of the $S_1 \leftarrow S_0$ transition, there is a shift to higher adiabatic ionization energy for Tol-d_3 compared to Tol-h_8, caused by larger isotopic shifts in the S_0 state compared to the ground cationic state.

To higher wavenumber in Figure 2, we have a band at 497 cm^{-1} for Tol-h_8. We can compare this value to the calculated ones in Table III, where it can be seen that there is very good agreement with the $\mathscr{M}_{29}^+$ vibrational wavenumber; however, reasonable agreement is also seen with the $\mathscr{M}_{11}^+$ value. The latter assignment is favoured as, under C_{2v} symmetry, the $\mathscr{M}_{29}^+$ vibration has b_2 symmetry (and so is formally forbidden), while the $\mathscr{M}_{11}^+$ vibration is allowed, and generally for the monosubstituted benzene cations, the strongest bands when exciting via the origin band are the totally symmetric ones. Additionally, the $\mathscr{M}_{29}^+$ vibration is observed in other spectra (see below) at a different wavenumber; indeed, a shoulder to the red of the main $\mathscr{M}_{11}^+$ band (labelled a/b in Figure 2) matches the assigned position of $\mathscr{M}_{29}^+$ (see later). In further support of the assignment of $\mathscr{M}_{11}^+$, in Tol-d_3 the corresponding feature is seen at 475 cm^{-1}, which matches the calculated wavenumber for $\mathscr{M}_{11}^+$ much better than that for $\mathscr{M}_{29}^+$. Additionally, the latter vibration is seen in other spectra at a different value, and, as with Tol-h_8, a shoulder is seen, this time to the blue of the main $\mathscr{M}_{11}^+$ band, matching the assigned position of $\mathscr{M}_{29}^+$.

To higher wavenumber, the weak band at 767 cm^{-1} may be identified with the $\mathscr{M}_{10}^+$ vibration; and an even weaker band at 980 cm^{-1} could be assigned to either $\mathscr{M}_8^+$ or $\mathscr{M}_9^+$, by comparison with the calculated wavenumbers; from evidence in later spectra, we assign this feature to $\mathscr{M}_8^+$. The first assignment is confirmed by the observation of a very weak feature at 747 cm^{-1} for Tol-d_3, which matches the calculated value very well; no corresponding feature is seen in the Tol-d_3 spectrum for the higher-wavenumber band (however, see later). There are a number of other weak features in the Tol-h_8 ZEKE spectrum, and we discuss their assignment below.

Looking at the calculated values, the band at 335 cm^{-1} could be due to either $\mathscr{M}_{30}^+$ or $\mathscr{M}_{14}^+$, both of which are forbidden under C_{2v} symmetry. We favour the assignment of the 335 cm^{-1} band to $\mathscr{M}_{14}^+$ mainly based on the fact that a very weak feature is seen in about the same position in the Tol-d_3 spectrum; the calculated frequencies indicate that the $\mathscr{M}_{14}^+$ vibration is not expected to shift significantly upon deuteration, in line with this assignment. Also, we note that the vibronic symmetry of these bands would then be $B_1 \times a_2 = B_2$, which is the same as the vibronic symmetry of the intermediate level ($B_2 \times a_1 = B_2$); however, as has been discussed elsewhere in relation to ZEKE spectra, and more generally in photoelectron spectroscopy, it is also possible for the departing photoelectron to contribute to the vibronic symmetry,[60] which would serve to make all bands vibronically allowed in this picture. We note also, that a weak shoulder to the blue of the $\mathscr{M}_{14}$ band in the Tol-h_8 spectrum is consistent with the position of the $\mathscr{M}_{30}^+$ band (see later).

At 377 cm^{-1}, there is a weak feature in the Tol-h_8 ZEKE spectrum, although a corresponding band could not be seen in the Tol-d_3 spectrum. This band may be assigned to $\mathscr{M}_{19}^+$ on the basis of the calculated wavenumbers in Table IV, which agrees with the assignment of a feature seen by Gunzer and Grotemeyer (when exciting via different intermediates, and labelled ν_{16b} therein)[43]—see later.

The feature at 530 cm^{-1} in the Tol-h_8 spectrum is not easily assignable to any fundamental, and in fact an assignment to the combination band $(\mathscr{M}_{19}\mathscr{M}_{20})^+$ matches the calculated wavenumber values well, and is a totally symmetric combination and so this assignment is favoured here. No corresponding band in the Tol-d_3 spectrum could be conclusively identified. This assignment, coupled with the $\mathscr{M}_{19}^+$ value

noted above, yields an approximate value for $\mathscr{M}_{20}^{+}$ of 153 cm^{-1}, which is in good agreement with the calculated value in Table IV.

There are also weak features seen at 566 and 733 cm^{-1} in the Tol-h_8 spectrum, which are consistent with assignments to $\mathscr{M}_{18}^{+}$ and $\mathscr{M}_{17}^{+}$, respectively, on the basis of the calculated values; only a corresponding $\mathscr{M}_{18}^{+}$ feature was observed in the Tol-d_3 spectrum.

We now compare to a number of other reports of photoelectron spectra of Tol-h_8. It is difficult to compare our Tol-h_8 ZEKE spectrum to the MPI-PES spectrum of Eisenhardt and Baumgärtel,[25] obtained when exciting via the origin, as the scale is quite compressed, and the resolution is much lower than that achieved in the present work. Bands below 1000 cm^{-1} at 411 cm^{-1}, 548 cm^{-1} and 831 cm^{-1} were noted, but it is difficult to find the correspondence of these to the present ZEKE spectrum. Similar comments regarding resolution apply to the MPI-PES spectrum of Meek *et al.*[35] obtained when exciting through the origin; however, here the progression with spacings of ∼480 cm^{-1} is likely $\mathscr{M}_{11}^{+}$, and it is possible that the spacings of ∼940 cm^{-1} are due to $\mathscr{M}_{8}^{+}$. Gunzer and Grotemeyer[43] obtained much better resolution when recording MATI spectra, which ought to give spectra equivalent to the ZEKE spectra, and we have referred to this work in the above. As well as internal rotor bands, they observed a vibration at 332 cm^{-1}, which they assign to $\mathscr{M}_{30}^{+}$ (Wilson mode 15 in that work); however, we disagree with that assignment ($\mathscr{M}_{30}^{+}$ will be assigned in Subsection IV B 3, but is seen as a shoulder on the high wavenumber side of the $\mathscr{M}_{14}^{+}$ band in Figure 2, as noted above). Whiteside *et al.*[37] report a number of bands below 1000 cm^{-1}, which were recorded via MPI-PES. An internal rotor band is observed at 45 cm^{-1}, but misassigned to the $3a_1'$ level, when this has been assigned to $3a_2''$ by Lu *et al.*[42] A band at 368 cm^{-1} is assigned to $\mathscr{M}_{30}^{+}$, but we assume this corresponds to the band we assign to $\mathscr{M}_{14}^{+}$ at 335 cm^{-1}, possibly overlapping with the 379 cm^{-1} band ($\mathscr{M}_{19}^{+}$), see above; a band at 496 cm^{-1} is assigned to $\mathscr{M}_{29}^{+}$, but we assign this to $\mathscr{M}_{11}^{+}$, a band at 540 cm^{-1} is assigned to $\mathscr{M}_{11}^{+}$, but we assume this is the band we observe at 530 cm^{-1}, assigned to a combination band. The band reported at 782 cm^{-1} in that work is likely the band we see at 747 cm^{-1}, and we agree with the assignment to $\mathscr{M}_{10}^{+}$ (denoted as Wilson mode 1 in Ref. 37). Finally, a band observed at 990 cm^{-1} in Ref. 37 and given two possible assignments therein, is likely the band we report at 980 cm^{-1}; one of the possible assignments given was to $\mathscr{M}_{8}^{+}$ with which we concur (see above).

3. 200–400 cm^{-1} region

This wavenumber region of the REMPI spectrum is shown in the upper trace of Figure 3 for both Tol-h_8 and Tol-d_3. We first address the assignment of the most intense band which appears at 331.4 cm^{-1} in the Tol-h_8 spectrum. It is at first striking that this band is at twice the wavenumber of the 165.1 cm^{-1} feature, suggesting that the latter could be a fundamental, and assignable as $\mathscr{M}_{20}$, with the 331.4 cm^{-1} feature being assigned as the overtone, $\mathscr{M}_{20}^{+}$; however, neither its position nor the shift of what appears to be the corresponding feature in the Tol-d_3 spectrum, at 294.6 cm^{-1}, is consistent

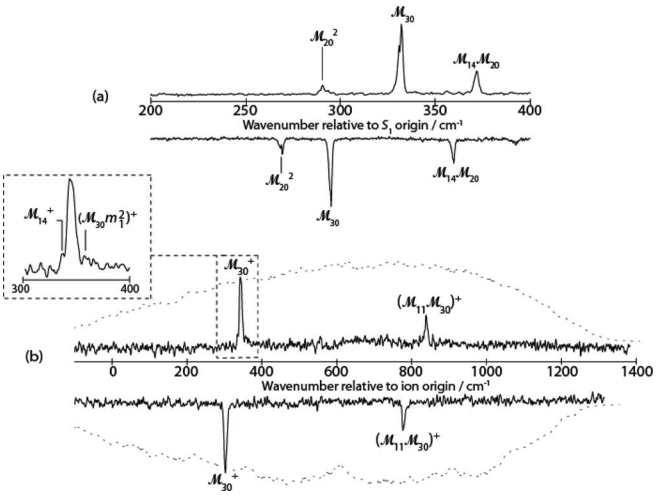

FIG. 3. (a) Expanded view of (1 + 1) REMPI spectra of Tol-h_8 (upright) and Tol-d_3 (inverted) in the range 200–430 cm^{-1}. (b) ZEKE spectra of Tol-h_8 (upright) and Tol-d_3 (inverted) via S_1 $\mathscr{M}_{30}^{1}$. The inset shows an expanded via of the $\mathscr{M}_{30}^{+}$ band in the Tol-h_8 ZEKE spectrum, indicating the weak, but reproducible, satellite bands. The dotted lines indicate the intensity of the uv light across the region.

with the calculated values for this vibration (see Table III). In Ref. 3, the 331.4 cm^{-1} feature is assigned to $\mathscr{M}_{30}$ on the basis of dispersed fluorescence spectra, which show a spectrum displaced from the origin spectrum by 344 cm^{-1}, consistent with previous experimental work on S_0, and both values are in reasonable agreement with the calculated wavenumbers (see Tables I and II). In the present work, we have excited via this feature and obtained a ZEKE spectrum, which is also shown in Figure 3. This clearly shows two bands, separated by the $\mathscr{M}_{11}^{+}$ vibrational wavenumber, with the more-intense, lower wavenumber feature at 342 cm^{-1} being assigned as the $\mathscr{M}_{30}^{+}$ vibration, consistent with the $\Delta v = 0$ propensity rule, and the higher band appears at 839 cm^{-1} (difference = 497 cm^{-1}) and being assigned as $(\mathscr{M}_{11}\mathscr{M}_{30})^{+}$. Note that a weak shoulder on the red side of the main $\mathscr{M}_{30}^{+}$ band (see inset of Figure 3) is in the correct position for $\mathscr{M}_{14}^{+}$, and compares well with the position of this feature when exciting via the origin (Figure 2). Additionally, a weak feature to the blue can be tentatively assigned as $(\mathscr{M}_{30}\, m_1^2)^{+}$; the lack of such a feature in Tol-d_3 would be consistent with the reduced rotational constant for internal rotation.

The dispersed fluorescence spectrum from Ref. 3, obtained from this same level, also shows both of these bands strongly, again with the $\Delta v = 0$ band being the more intense. Additionally, when we compare the Tol-d_3 ZEKE spectrum to the Tol-h_8 one, we see the expected corresponding activity, with the $\mathscr{M}_{30}^{+}$ band at 303 cm^{-1}, and the $(\mathscr{M}_{11}\mathscr{M}_{30})^{+}$ band at 777 cm^{-1} (difference of 474 cm^{-1}, matching that expected for $\mathscr{M}_{11}^{+}$). Good agreement with the $\mathscr{M}_{30}^{+}$ calculated vibrational wavenumbers (Table III) is seen.

Only one other group has recorded photoelectron spectra when exciting via this S_1 feature, which was Whiteside *et al.*[37] The two main bands were reported at 360 cm^{-1} and 834 cm^{-1}, and these must correspond to the bands observed in the present work at 343 cm^{-1} and 839 cm^{-1}. Although we concur with the assignment of the lower-wavenumber fea-

ture to $\mathscr{M}_{30}^{+}$, we do not concur that it is the same feature as seen when exciting via the origin (see above); nor do we agree with their assignment of the higher wavenumber band as $(\mathscr{M}_{29}\mathscr{M}_{30})^{+}$, but rather our deuterated results show that it is $(\mathscr{M}_{11}\mathscr{M}_{30})^{+}$, as discussed above.

We now move on to discuss the two features observed at 289.9 cm^{-1} and 371.0 cm^{-1} in Tol-h_8 and at 268.9 and 359.2 cm^{-1} in Tol-d_3. The 371.0 cm^{-1} feature in the Tol-h_8 spectrum was also seen in the fluorescence study by Hickman *et al.*[3] who dispersed the fluorescence, finding a spectrum displaced from that of the origin by 604 cm^{-1}; they assigned this band as $\mathscr{M}_{14}\mathscr{M}_{20}$. This feature was also seen by Murakami *et al.*[27] and is evident in the spectrum of Doyle *et al.*[24] Persual of Table II shows that both this and the 289.9 cm^{-1} feature are likely associated with the two lowest-wavenumber fundamentals, $\mathscr{M}_{14}$ and $\mathscr{M}_{20}$. Clearly neither fundamental can be attributed to this feature, on the grounds of both wavenumber and symmetry; however, combinations and overtones are possible. We concur with the assignment by Hickman *et al.*[3] of the 371.0 cm^{-1} band as the $\mathscr{M}_{14}\mathscr{M}_{20}$ combination band (b_2 symmetry, vibronically allowed). This then implies that the 289.9 cm^{-1} feature is due to an overtone. We note that this feature appears to be present in the fluorescence excitation spectrum of Doyle *et al.*[24] and may be the same feature as the one observed at 281 cm^{-1} by Kahane-Paillous and Leach.[18] The $\mathscr{M}_{14}^{2}$ overtone would be expected to be >400 cm^{-1} and so it seems most likely that the 290 cm^{-1} band is due to $\mathscr{M}_{20}^{2}$. These assignments then suggest values of 226 and 145 cm^{-1} for $\mathscr{M}_{14}$ and $\mathscr{M}_{20}$, respectively. The corresponding bands in the Tol-d_3 spectrum lie at 268.9 and 359.2 cm^{-1}, with the same rationale leading to values of 225 and 134 cm^{-1} for $\mathscr{M}_{14}$ and $\mathscr{M}_{20}$, respectively. We note that this suggests that the wavenumber of $\mathscr{M}_{14}$ is largely unchanged by deuteration, in line with the calculated values, and the form of the vibrational mode; on the other hand, the $\mathscr{M}_{20}$ band is decreased significantly upon deuteration, again in line with the calculated values, and the form of the vibrational mode. As mentioned above, we have discussed a possible assignment of the 165 cm^{-1} band (labelled ξ in Figure 2) to the fundamental, $\mathscr{M}_{20}$, but with large anharmonicity in overtones and combinations, but we cannot be definitive regarding the assignment of this band. We suspect, in concurrence with suggestions by Gascooke and Lawrance from Flinders University, Adelaide, Australia, that this feature could in fact be an internal rotor level shifted by vibration-torsional coupling via interactions with close-lying vibrational levels (or possibly the $\mathscr{M}_{20}$ shifted by a similar mechanism); the same comments refer to the Tol-d_3 feature (marked ξ' in Figure 2).

We did not record ZEKE spectra via the bands at 289.9 and 371.0 cm^{-1} for Tol-h_8, nor the corresponding Tol-d_3 bands, owing to their low intensity; clearly such spectra would help in confirming the suggested assignments.

4. 400–500 cm^{-1} Fermi resonance region

We show the region of the REMPI spectrum between 400 and 500 cm^{-1} in the upper trace of Figure 4 for both Tol-h_8 and Tol-d_3. First, we note that the weak feature at 431.0 cm^{-1} in the Tol-h_8 spectrum was apparently not observed by Hickman *et al.*[3] It seems to have a counterpart in the Tol-d_3 spectrum at 412.2 cm^{-1}. One possible assignment of these features is to $\mathscr{M}_{20}^{3}$, which would appear at 435 cm^{-1} and 403 cm^{-1}, for Tol-h_8 and Tol-d_3, respectively, based upon 1.5 times the wavenumber of the bands assigned as $\mathscr{M}_{20}^{2}$. Such an assignment would, however, require significant and unusual anharmonic effects. Another possibility arises from the calculated values in Table III, which suggest that these features could be associated with the $\mathscr{M}_{18}$ vibration, which shows a moderate change in wavenumber upon deuteration. However, based on LIF spectra from Doyle *et al.*[24] our favoured assignment is actually to the toluene-Ar complex, which is expected to have shifts of ~25 cm^{-1} relative to the band arising from the corresponding uncomplexed molecule. The band at 431.0 cm^{-1} is in the correct position for the analogue of the lowest Fermi resonance feature in (Tol-h_8)-Ar and is denoted $\overline{M_{11}}$, although this feature may be in Fermi resonance (see below). Assuming similar shifts for the deuterated species, the band in Tol-d_3 at 412.2 cm^{-1} is also at the correct wavenumber for the corresponding feature. Given the close agreement of both features to the expected position, these seem reasonable assignments for these features. We note that Doyle *et al.*,[24] who only studied Tol-h_8, also saw a band shifted 20 cm^{-1} to the red of the second Fermi resonance feature, which was unexpected as all other shifts were consistent at 25 cm^{-1}. No explicit explanation for the shift was given—if the assignment to the second main Fermi resonace component is correct, then this may be symptomatic of the different interactions occurring for these vibrations; if the feature is something else, then it suggests that the expected second Fermi resonance feature is absent, perhaps explainable from different interactions upon complexation. We did not record spectra via this feature for either Tol-h_8 or Tol-d_3, owing to its low intensity. The explanation for the appearance of this feature in our mass-resolved spectrum is that the complex undergoes rapid vibrational predissociation, as ascertained in LIF experiments by Da Campo and Mackenzie;[61] in that work they observed fluorescence characteristic of the uncomplexed toluene molecule after having exciting on a toluene-Ar resonance, indicating that the predissociation is rapid.

As noted above, in the Tol-h_8 spectrum, there is a complicated set of features in the range 450–475 cm^{-1}, which can be seen in the top trace of Figure 4. In the centre, there are two strong peaks at 456.6 cm^{-1} and 462.2 cm^{-1}, with other weaker bands close by, some of which may be due to the partially resolved rotational profile. To higher and lower wavenumber there are weaker bands at 472.6 cm^{-1} and 451.8 cm^{-1}. In previous work, the assignment of the two most intense features to a Fermi resonance has been made;[3,54] however, it is clear from other spectra,[24,54] and those presented here, that this region contains more than one contribution. Indeed, very recent time-resolved work (to be discussed further below), reports evidence for three contributions to the Fermi resonance.[41] In early work,[54] the two most intense features were assigned as being in Fermi resonance, but only one component was explicitly assigned (as $\mathscr{M}_{11}$). In Ref. 3 the Fermi resonance was deduced as arising from an interaction between

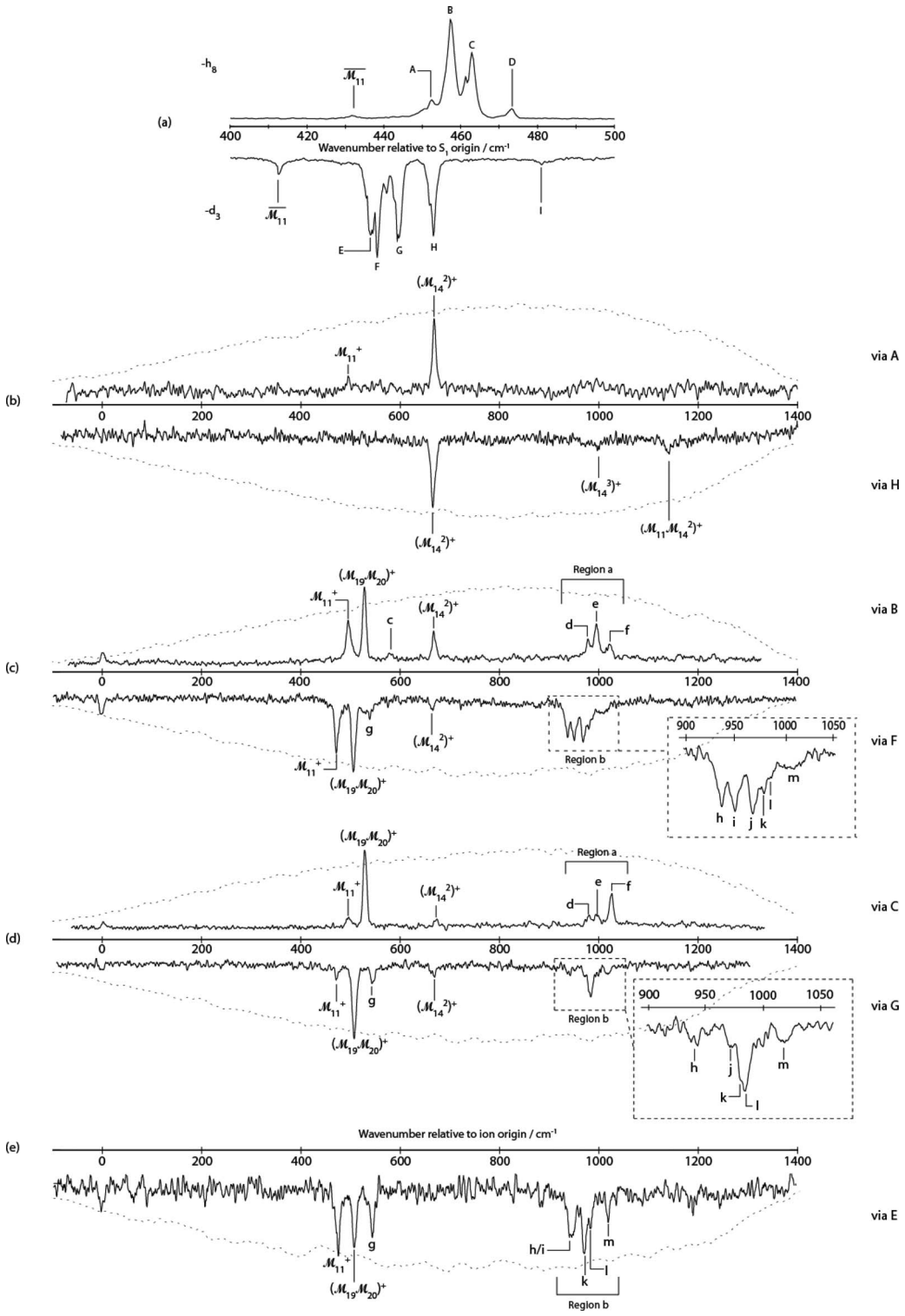

FIG. 4. (a) Expanded view of the Fermi resonance region of the (1 + 1) REMPI spectra of Tol-h_8 (upright) and Tol-d_3 in the range 430–480 cm^{-1}. Traces (b)–(e) contain ZEKE spectra recorded via eigenstates designated by the letters in the top trace of the REMPI spectrum. Spectra for Tol-h_8 and Tol-d_3 have been paired up based on their appearance and assignment: see text. The assignment of bands marked with letters are discussed in the text. The dotted lines indicate the intensity of the uv light across the region.

the $\mathscr{M}_{11}$ and $\mathscr{M}_{19}\mathscr{M}_{20}$ vibrations, with the interaction leading to strong mixing of the modes. For this reason, we refrain from referring to the bands by an explicit vibrational assignment, and instead have labelled the main four features in the Tol-h_8 spectrum, A–D. For the first time, we also present the same region of the spectrum for Tol-d_3, and again it may be seen to have a similar complicated appearance. However, the contributions and mixings are expected to be different as the vibrations are now at different relative wavenumbers, but still close enough to expect interaction. Again, we identify (at least) four contributions, and label these features E–H.

In the lower traces of Figure 4, we show ZEKE spectra recorded via each of the strong features. What was immediately noticeable when comparing the Tol-h_8 and Tol-d_3 ZEKE spectra was that, as expected, there was similar vibrational activity observed when exciting via these features, as expected for vibrations in Fermi resonance, and as observed in the dispersed fluorescence spectra recorded from the two most intense features.[3] In addition, it is striking that the observed activity in a Tol-h_8 ZEKE spectra is matched by that observed in a Tol-d_3 one; this turns out to be a powerful aid in tracking which bands in the Tol-h_8 Fermi resonance feature match up with which bands in the Tol-d_3 one. In Figure 4, we have anticipated our conclusions by presenting the Tol-h_8 ZEKE spectra paired up with their corresponding Tol-d_3 one; additionally, we summarize the positions of each of the main observed features in Table VII. We now discuss the assignment of the REMPI and ZEKE spectra in the light of the results from the dispersed fluorescence spectra of Ref. 3, our quantum chemical results for the two isotopologues, and the assignments of lower wavenumber features already given.

We note that previous assignments of this region for Tol-h_8 have assigned the bands at 456.6 and 461.8 cm^{-1} to strongly mixed $\mathscr{M}_{11}$ and $\mathscr{M}_{19}\mathscr{M}_{20}$ vibrations; in particular, the authors of Ref. 3 discussed this assignment, and appear to be the first to suggest the particular combination band interacting with $\mathscr{M}_{11}$. The identification of a Fermi resonance between these features is made by noting the appearance of S_0 vibrations corresponding to each contributor state, in each of the two recorded dispersed fluorescence spectra. These bands, labelled B and C in Figure 4, indeed have ZEKE spectra which each show activity in two vibrations to low wavenumber. The band in the ZEKE spectra, which is the more intense in both cases, has a wavenumber of 528 cm^{-1}—consistent with its assignment to $(\mathscr{M}_{19}\mathscr{M}_{20})^+$, based upon the calculated vibrational wavenumbers (see Table III) for these two vibrations. The lower wavenumber feature has a value which is consistent with the calculated vibrational wavenumber of $\mathscr{M}_{11}^+$. Hence, the ZEKE results on these two bands confirm the assignment[3] of bands B and C in the REMPI spectrum to eigenstates which are strong mixtures of $\mathscr{M}_{11}$ and $\mathscr{M}_{19}\mathscr{M}_{20}$. It may also be noted that there is a band in the ZEKE spectrum to higher wavenumber at 669 cm^{-1}. This band is seen cleanly when exciting via band A. Inspection of the calculated frequencies for the cation (Table IV) show that a viable assignment of this feature is to $(\mathscr{M}_{14}^2)^+$, with the fundamental wavenumber being estimated as 335 cm^{-1}, in agreement with the value discussed earlier in relation to the ZEKE spectrum recorded via $S_1 0^0$. Recently, the 451.8 cm^{-1} band in the REMPI spectrum has also been suggested as being assignable to $\mathscr{M}_{14}^2$ and being in Fermi resonance with the $\mathscr{M}_{11}$ and $\mathscr{M}_{19}\mathscr{M}_{20}$ vibrations in S_1,[41] and the present results confirm this. It is interesting to note that only the $\mathscr{M}_{11}^+$ band appears with $(\mathscr{M}_{14}^2)^+$ in the ZEKE spectrum recorded via band A, with the $(\mathscr{M}_{19}\mathscr{M}_{20})^+$ band being absent, suggesting that $\mathscr{M}_{14}^2$ is more strongly coupled to $\mathscr{M}_{11}$ in the S_1 state than to the $\mathscr{M}_{19}\mathscr{M}_{20}$ combination. We note that the three features in the ZEKE spectrum are over 30 cm^{-1} apart from each other, with the $(\mathscr{M}_{14}^2)^+$ band being over 130 cm^{-1} to higher energy: thus, the corresponding vibrations are unlikely to be in strong Fermi resonance, as they are in the S_1 state.

When exciting though band B, we also observe a band at 579 cm^{-1}. First, we note that in the REMPI spectrum, the profiles of bands B and C are quite different, and one might conclude they are of different symmetries; however, it is clear from previous work, particularly the dispersed fluorescence results[3] and the ZEKE results presented here, that these two bands arise from Fermi resonance coupled states. This suggests that there may be another feature under band B, "filling in" the band gap. There is no obvious fundamental or combination band which would appear in this region, but it is possible that vibration-internal rotor combination bands may contribute. We note that Gascooke and Lawrance[44] calculate that the $\mathscr{M}_{14}\mathscr{M}_{20}$ ($m = 4$) band should appear in this region at ~457 cm^{-1}, which has the correct symmetry (totally symmetric). This would place it very close to the $\mathscr{M}_{11}$ band and so it also could be responsible for the "filling in" of the rotational profile. Assuming this feature is also overlapped when exciting through band B, then we would expect to see a ZEKE feature corresponding to the cationic wavenumber. This is predicted to arise at ~571 cm^{-1}, not too far removed from the observed band at 579 cm^{-1}; as noted above these bands could be interacting in the cation and so be shifted from their expected positions. The proximity of this feature would explain why it only appears when exciting through band B. However, this assignment has two key flaws: first, there is no evidence from the time-resolved study[41] that another coupled level exists so close to the $\mathscr{M}_{11}$ state; and secondly, there is no evidence in the 2D-LIF[44] study for such an additional feature.

We thus consider an alternative assignment. As will be discussed later, when referring to the time-resolved experiments of Davies *et al.*[41] it has been hypothesized that the Fermi resonance feature is, in fact, made up of three main vibrational contributors, each of which has $m = 0$ and $m = 1$ components. Furthermore, Gascooke and Lawrance[44] have shown that these vibration-torsion levels are each interacting with other vibration-torsion levels, but to differing extents. As discussed therein, in the case of band B, this is made up of $m = 0$ and $m = 1$ components, which have been shifted enough to lead to an obscuring of the band gaps of each feature. The shifts for band C are smaller, and so the band gap is still clearly visible, as is seen on (say) the origin band. Since the corresponding states are much further apart in the cation, then the interactions are smaller and so in the ZEKE spectrum we cannot resolve the different m^+ contributions, and so these appear as single bands.

The "extra" band at 579 cm^{-1} is intriguing, this lies 31 and 51 cm^{-1} above bands B and C, respectively; as such, this could be assigned as $(\mathscr{M}_{19}\mathscr{M}_{20}\ m = +3)^+$, which would be expected at this wavenumber; it would then be surprising that the $(\mathscr{M}_{11}\ m = +3)^+$ band is not observed, which would be expected close to 547 cm^{-1}—plausibly it is obscured under the high wavenumber tail of the main $(\mathscr{M}_{19}\mathscr{M}_{20})^+$ band. Neither of these bands is totally symmetric; however, we note that the $m = +3$ band is seen clearly when exciting via the origin, where it is also symmetry forbidden. The appearance of such bands may be attributed to vibronic-torsional couplings,

although the symmetry of the departing electron may also play a role.

We now compare to the corresponding spectra obtained for Tol-d_3. As noted, we have paired together the ZEKE spectra for Tol-h_8 and Tol-d_3 that resemble each other. Their appearance immediately tells us that feature F in the Tol-d_3 REMPI spectrum has an assignment that corresponds to that of band B in Tol-h_8; similarly, band G in the Tol-d_3 REMPI spectrum has an assignment that corresponds to that of band C in Tol-h_8. We can see that, indeed, the activity observed is similar, and comparison with the calculated cationic vibrations in Table III supports the same assignment of the low wavenumber features. We also note that the shifts in the S_1 wavenumbers for these assignments are in line with expectations based on the calculated isotopic shifts from the values given in Table III. Also of note is that a weak band assignable to $(\mathscr{M}_{14}^{\ 2})^+$ is seen when exciting through both bands F and G; further, when exciting through band H, we see a single feature to low wavenumber, which is again assignable to $(\mathscr{M}_{14}^{\ 2})^+$. Notably, we see no features corresponding to $\mathscr{M}_{11}^{\ +}$ nor $(\mathscr{M}_{19}\mathscr{M}_{20})^+$ in this particular spectrum. We shall discuss the activity observed in these spectra further below. The correspondence of features A and H to $\mathscr{M}_{14}^{\ 2}$ for Tol-h_8 and Tol-d_3 is in line with the expectation that this vibration is highly insensitive to deuteration, both in the S_1 state (see Table II) and in the cation (Table III).

Looking back at the REMPI spectrum traces for the Fermi resonance regions at the top of Figure 4, we note that there is an additional feature to high wavenumber (band D) for Tol-h_8, and also a feature to low wavenumber in the spectrum for Tol-d_3 (band E). Unfortunately, a ZEKE spectrum was not recorded for band D, in part owing to its low intensity. A reasonable assignment of this band, however, could be to $\mathscr{M}_{20}\mathscr{M}_{30}$, which would have a predicted wavenumber of 476 cm^{-1} based upon the sum of the wavenumbers of the individual contributing vibrations; this is reasonable agreement, considering anharmonic shifts. If we consider where this feature would arise for Tol-d_3, we see that this would be at around 429 cm^{-1} and so suggestive of an assignment of band E to this vibration. Such bands would have ($b_1 \times b_2 = a_2$) vibrational symmetry, and so $B_2 \times a_2 = B_1$ vibronic symmetry, and so be symmetry forbidden. Another possibility is the $\mathscr{M}_{18}$ ($m = -3$) vibration-internal rotation band, which we estimate will occur at 470–475 cm^{-1}; note the sign of the $m = 3$ level is required to be negative to give a totally symmetric combination with the $\mathscr{M}_{18}$ vibration. This feature could then interact with the other states, in a manner described by Gascooke and Lawrance.[44] Since we recorded a ZEKE spectrum for band E, presented as the bottom trace in Figure 4, we examine this for further insight.

The spectrum shows three distinct features in the low wavenumber region, with two of these straightforwardly identifiable as the $\mathscr{M}_{11}^{\ +}$ and $(\mathscr{M}_{19}\mathscr{M}_{20})^+$ features seen when exciting via the two most intense contributors to the S_1 Fermi resonance. The third feature at 542 cm^{-1} is somewhat more difficult to assign. One of the suggested assignments of band E was to $\mathscr{M}_{20}\mathscr{M}_{30}$. If this were correct, then the $\Delta v = 0$ rule would suggest we should see a band corresponding to the $(\mathscr{M}_{20}\mathscr{M}_{30})^+$ vibration at ∼443 cm^{-1} and there are no features below the 473 cm^{-1} band. This suggests that band E requires a different assignment. Noting the suggested assignment of band D to the $\mathscr{M}_{18}(m = -3)$ band for Tol-h_8, we estimate that the corresponding feature in Tol-d_3 should appear at ∼430 cm^{-1}, which is reasonably close to the peak position of band E. Additionally, we note that the expected value for $[\mathscr{M}_{18}(m = -3)]^+$ is 546 cm^{-1}, which is close to the position of the additional band at 542 cm^{-1}. Given the fact that bands arise from interacting vibrations and vibration-internal rotation coupling, we currently accept this assignment. We note that this additional ZEKE band is seen with the highest relative intensity when exciting via band E, but can also be seen clearly when exciting via band G and weakly when exciting via band F, suggesting the originating state is coupled to both $\mathscr{M}_{11}$ and $\mathscr{M}_{19}\mathscr{M}_{20}$ in the S_1 state. It is interesting to note the high relative intensity of band H in the Tol-d_3 spectrum compared to the corresponding band A in that of Tol-h_8. We shall comment on this further in the below.

Comparing to previous spectra, we note that Gunzer and Grotemeyer[43] recorded MATI spectra via what appears to have been the 456.6 cm^{-1} feature of the Fermi resonance feature, which they associate solely with the $\mathscr{M}_{11}$ vibration, even though their REMPI spectrum clearly shows a complicated structure with features the same as reported herein, and as had been seen by previous workers (see above). As here, Gunzer and Grotemeyer observe two clear features at around 500 cm^{-1}, but they associate these with $\mathscr{M}_{11}^{+}$ and $\mathscr{M}_{29}^{+}$; our discussion above clearly disagrees with the latter assignment. It is notable that no reference to the work of Hickman *et al.*[3] was made in that work, where an assignment of the Fermi resonance feature was given. Interestingly, Gunzer and Grotemeyer[43] report a MATI spectrum via the S_1 $\mathscr{M}_{29}$ band, but did not assign the features therein. We discuss the assignments of these bands in the below. These authors also observed very weak features at 332 and 379 cm^{-1}, which they assign to Varsányi modes 15 and 16b ($\mathscr{M}_{30}$ and $\mathscr{M}_{19}$ here, respectively). We have already noted our disagreement with the assignment of the lower wavenumber feature, in the above; the 379 cm^{-1} band was also noted as being observed when exciting via the internal rotor band $m = +3$ in Ref. 43. We have already agreed with the assignment of the latter to $\mathscr{M}_{19}^{+}$, which we observe weakly when exciting via $S_1 0^0$. Whiteside *et al.*[37] reported spectra when exciting through one of the Fermi resonance features, observing a main progression in the $\mathscr{M}_{11}^{\ +}$ vibration as well as other bands. Although their reported wavenumbers are different to ours, this seems largely attributable to estimating the position of a broad band from their less well resolved spectra. It is difficult to be definitive of precisely where in the Fermi resonance feature they excited, but the observation of the $\mathscr{M}_{11}^{+}$ progression, together with the fact that the lower wavenumber feature is the more intense of the two main components, suggests the latter was the point of excitation. Clearly the wavenumbers reported here are the more reliable, owing to the narrower bands obtained.

We now turn to the higher wavenumber features observed in the ZEKE spectra shown in Figure 4, concentrating first on Tol-h_8. First, the spectra obtained via band A and H only show weak features to high wavenumber in the case of

Tol-d_3. One of these, at 997, cm^{-1} can be reasonably assigned to $(\mathscr{M}_{14}^{3})^{+}$, while the 1139 cm^{-1} feature is straightforwardly assigned as the combination band $(\mathscr{M}_{11}\mathscr{M}_{14}^{2})^{+}$. If we consider the high-wavenumber end of the spectra recorded for Tol-h_8 via bands B and C, we see three features in each case which we label Region a, containing individual bands labelled d–f, with band e being the most intense when exciting via band B and band f being the most intense when exciting via band C; band d has similar intensity in both cases. Comparison with the assignment of the lower wavenumber region suggests assignment of band e as $(\mathscr{M}_{11}^{2})^{+}$ and band f as $(\mathscr{M}_{11}\mathscr{M}_{19}\mathscr{M}_{20})^{+}$. The assignment of band d, at 979 cm^{-1}, can be made by reference to the calculated cationic wavenumbers in Table IV, suggesting $\mathscr{M}_{8}^{+}$. With regard to the corresponding spectral region of Tol-d_3, this can be seen to be more complicated, with five different features in a narrow range, labelled Region b. By comparison with the low wavenumber region, the observed behaviour of the bands when exciting via bands B and C for Tol-h_8, and the behaviour of the bands in this region, the following two bands are expected in this region: $(\mathscr{M}_{11}^{2})^{+}$ and $(\mathscr{M}_{11}\mathscr{M}_{19}\mathscr{M}_{20})^{+}$. Band k is likely to be $(\mathscr{M}_{11}\mathscr{M}_{19}\mathscr{M}_{20})^{+}$ from its dominance of this region when exciting via band G; band i is more difficult, as this could also be assigned to $(\mathscr{M}_{29}^{2})^{+}$. However, the fact that band h appears with about the same intensity when exciting via both bands F and G, plus the fact that the calculated wavenumber for $\mathscr{M}_{29}$ is higher than that of $\mathscr{M}_{11}$, suggests band i should be assigned as $(\mathscr{M}_{29}^{2})^{+}$ and band h as $(\mathscr{M}_{11}^{2})^{+}$. The observation of $\mathscr{M}_{8}^{+}$ in the case of Tol-h_8, plus the calculated shift in wavenumber, suggests that band j should be assigned as $\mathscr{M}_{8}^{+}$ for Tol-d_3. The broadness of band k, plus its changing profile between the two spectra suggests it may have another contribution, and we note that $\mathscr{M}_{9}^{+}$ has a calculated value in this region, which we tentatively assign as contributing to this feature (represented by the label l). Finally, the rather broad feature, labelled as band m has the correct wavenumber to be the $[\mathscr{M}_{11}\mathscr{M}_{18}\ (m = -3)]^{+}$ combination band. The high wavenumber region of the spectrum obtained when exciting via band E shows features which have already been assigned.

Some of the features at this end of the spectrum are close in wavenumber, and so it is likely that these are interacting via Fermi resonance or via Darling-Dennison resonance[62]—the latter would apply to interactions between $\mathscr{M}_{11}^{2}$ and $\mathscr{M}_{29}^{2}$, whose fundamentals do not have the correct (C_{2v}) symmetry to interact, but which can interact in the overtone region, where both are now totally symmetric. Likewise, although the lower wavenumber features are more removed in energy, there could be some interaction between them, which has pushed them apart. This, and/or different photoionization cross-sections, could be responsible for the fact that the $\mathscr{M}_{11}^{+}$ band is not the most intense feature in that region (see further comments below).

Additionally, we recorded spectra through the low wavenumber side of band C (spectra not shown), but these showed the same spectrum as exciting through the higher wavenumber side; however, we did not attempt spectra exciting through the centre or low wavenumber side of band B; however, as noted above, we would not expect to observe any significant difference in this region of the ZEKE spectra from exciting through $m = 0$ and $m = 1$ features. There is the possibility, however, of searching for such differences by monitoring the internal rotor levels which appear on the main origin band, and here one may expect to observe enhanced intensities in bands such as m_1^2; this could be the subject of a further study.

Finally, a very weak band at 480.6 cm^{-1} in the REMPI spectrum of Tol-d_3 is assignable to the $\mathscr{M}_{14}^{2}$ ($m = +3$) level. It is intriguing that there are no obvious bands which correspond to the $\mathscr{M}_{11}$ ($m = +3$) or $\mathscr{M}_{19}\mathscr{M}_{20}$ ($m = +3$) levels; this will be discussed further in the following subsection.

5. 500–700 cm^{-1} region

The REMPI spectra for both Tol-h_8 and Tol-d_3 in this wavenumber region are shown in the upper traces of Figure 5. The dominant feature in this spectral region for Tol-h_8 is the band at 531.3 cm^{-1}, which has previously been assigned to $\mathscr{M}_{29}$, consistent with the results from dispersed fluorescence experiments.[3] A corresponding feature in the Tol-d_3 spectrum may be seen to appear at 529.1 cm^{-1}. We note that Gascooke and Lawrance[44] have been able to show that this feature is made of slightly displaced components arising from $m = 0$ and $m = 1$, to which we are not sensitive in the ZEKE spectrum.

Our ZEKE spectra recorded when exciting through these features are shown in Figure 5, where it is noteworthy that the strong bands close to 480 cm^{-1} in each case have a width close to twice that of the other features, suggesting that they consist of more than one contribution. This is particularly clear in the case of Tol-h_8, where a clear shoulder on the low wavenumber side of the main peak can be seen, with the lower wavenumber feature at 477 cm^{-1}, and the main peak at 486 cm^{-1}. There are other features to higher wavenumber, and these will be discussed further below.

Considering Tol-h_8 first, one of the two low wavenumber features in the ZEKE spectrum, labelled a and b in Figure 5 (where the overall feature is seen as a weak shoulder in Figure 2 and labelled a/b therein), is clearly associated with $\mathscr{M}_{29}^{+}$, and the $\Delta v = 0$ rule initially suggests the more intense feature at 486 cm^{-1} should be assigned to this. Assignment of the second feature is less straightforward, with no obvious fundamental of b_2 symmetry being a likely candidate. We thus pursue an assignment in terms of a combination band, and conclude that $(\mathscr{M}_{14}\mathscr{M}_{20})^{+}$ is the most likely. This combination has $a_2 \times b_1 = b_2$ symmetry and so is formally allowed when exciting through the $S_1\mathscr{M}_{29}$ intermediate state, under C_{2v} symmetry. We note that we have assigned wavenumbers of 335 cm^{-1} and 153 cm^{-1} to $\mathscr{M}_{14}^{+}$ and $\mathscr{M}_{20}^{+}$ vibrations in the above, giving a combination value of 488 cm^{-1}. If we then compare this with the corresponding Tol-d_3 spectrum, we see a single band, but also with about twice the width of the other features in the spectrum. If we calculate where the $(\mathscr{M}_{14}\mathscr{M}_{20})^{+}$ combination will be, we obtain a value of 478 cm^{-1}, which is very close to the measured position of the main band (477 cm^{-1}). We conclude that this feature consists of two very close features, which are likely

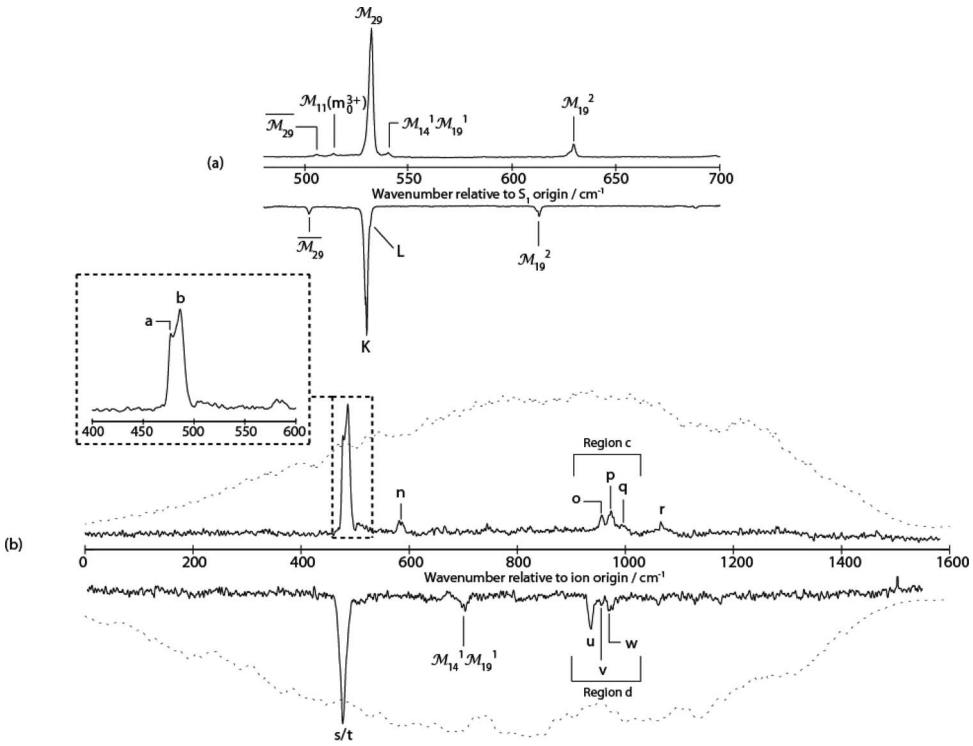

FIG. 5. (a) Expanded view of (1 + 1) REMPI spectra of Tol-h_8 (upright) and Tol-d_3 (inverted) in the range 480–700 cm^{-1}. (b) ZEKE spectra of Tol-h_8 (upright) and Tol-d_3 (inverted) via S_1 $\mathscr{M}_{29}^1$. The inset shows the main band for Tol-h_8 is composed of two components. The assignment of bands marked with letters are discussed in the text. The dotted lines indicate the intensity of the uv light across the region.

to be in Fermi resonance. If we now look at the calculated values for $\mathscr{M}_{29}^+$ for both Tol-h_8 and Tol-d_3 we see that we would expect them to be very similar; indeed the calculations suggest that the Tol-d_3 value may be slightly higher. Referring to the values for the S_0 state we see that the experimental values are the same, i.e., there is no shift upon deuteration, although the calculated Tol-d_3 value is lower than the Tol-h_8 one. We again conclude that these values should be very close for the cation also. We note that, in the earlier dispersed fluorescence study,[3] there was no evidence for Duschinsky rotation or Fermi resonance effects in the S_1 state, and so our results would be consistent with interactions occurring in the cation.. Owing to the similar intensities of the two peaks in the Tol-h_8 spectrum, the two vibrations are likely to be strongly coupled, and therefore best described by a linear combination of the two proposed zero-order vibrations, We also note that, at 974 cm^{-1}, a band is seen which would correspond to the combination band $(\mathscr{M}_{11}\mathscr{M}_{29})^+$, and that such a band is seen in chlorobenzene,[67] for example. Such combinations with the $\mathscr{M}_{11}^+$ mode are commonplace in substituted benzene spectra. Oddly, it is not possible to identify a corresponding feature in the Tol-d_3 spectrum; indeed, we find that the remainder of the bands in this wavenumber region (marked region c for Tol-h_8 and region d for Tol-d_3) are difficult to assign with any certainty for both Tol-h_8 and Tol-d_3. It may be seen, by comparing with the high wavenumber region of the spectra in Figure 4 when exciting via the S_1 Fermi resonance features at ∼460 cm^{-1} (see above), that there are a number of features possible in this region; however, a definitive assignment was not possible, and we attribute this to the effects of anharmonicity, Fermi and Darling-Dennison resonances and vibronic interactions.

The small band (likely more than one band) to the high wavenumber side of the main band in the Tol-h_8 ZEKE spectrum, located at 504 cm^{-1} may be due to an internal rotational transition (such as m_1^2) combined with the main peaks, or may arise from combination bands shifted by anharmonicity; the former seems the more likely as such a band is not observed for Tol-d_3, where the shift in internal rotor energy would lead to the band being too close to the main one to be observed. An assignment of the band at 581 cm^{-1} (labelled "n") is also required. Interestingly, it matches the expected wavenumber of $\mathscr{M}_{19}\mathscr{M}_{20}$ ($m = +3$) very well, although it might then have been expected to see the $\mathscr{M}_{11}$ ($m = +3$) band at ∼525 cm^{-1}, which is not clearly present, although it could be part of the feature appearing to the blue side of the main ZEKE band at 477/486 cm^{-1}. There are no obvious features in the Tol-d_3 spectrum corresponding to these assignments. A feature at ∼703 cm^{-1} in the Tol-d_3 spectrum is tentatively assigned to $(\mathscr{M}_{14}^1\mathscr{M}_{19}^1)^+$. This observation would be consistent with the $\mathscr{M}_{14}\mathscr{M}_{19}$ band being a shoulder on the main $\mathscr{M}_{29}$ band in the REMPI spectrum of Tol-d_3, and so co-excited with $\mathscr{M}_{29}$, or as in the case of chlorobenzene, the two vibrations may be in Fermi resonance in the S_1 electronic state.

Although the work here appears to be the first to record spectra for Tol-d_3^+ via resonant ionization, previous workers have used the S_1 $\mathscr{M}_{29}$ level of Tol-h_8 as an intermediate in recording such spectra. Meek *et al.*[35] recorded a time-of-flight photoelectron spectrum, observing vibrational spacings of 480 cm^{-1}, which are likely attributable to the

$\mathscr{M}_{29}^{+}$ vibration, as noted here, but with the series possibly also containing contributions from combination bands involving both $\mathscr{M}_{11}^{+}$ and $\mathscr{M}_{29}^{+}$. Gunzer and Grotemeyer, in their MATI study,[43] also saw a feature which has a double peak, at 477 and 485 cm^{-1}: these values match those here very well. As noted above, no assignment of these bands was given in that work, even though the assignment of at least one of these features to $\mathscr{M}_{29}^{+}$ on the basis of the $\Delta v = 0$ rule should have been facile. Unfortunately, however, these authors incorrectly assigned $\mathscr{M}_{29}^{+}$ to a higher wavenumber feature seen when exciting through the most intense component of the Fermi resonance feature (see above). This misassignment seems to have arisen both from the neglect of the $\Delta v = 0$ rule, lack of consideration of symmetry, and having not referred to the work of Hickman *et al.*[3] The later work on resonant laser photoelectron spectroscopy by Whiteside *et al.*[37] only observed a single feature in this region, reported at 496 cm^{-1}, when exciting via the $\mathscr{M}_{29}$ level, assigned to the $\mathscr{M}_{29}^{+}$ vibration; other (unassigned) features were also seen to higher wavenumber.

There are other features seen in the REMPI spectrum in the top trace of Figure 5, but we did not record ZEKE spectra via these features, owing to their low intensity. The second most-intense band is located at 628.5 cm^{-1} for Tol-h_8 and at 612.3 cm^{-1} for Tol-d_3. There is no obvious assignment of this band in terms of a fundamental; however, there is a straightforward assignment as the $\mathscr{M}_{19}$ overtone, yielding approximate values for $\mathscr{M}_{19}$ in S_1 of 314 and 306 cm^{-1} for Tol-h_8 and Tol-d_3, respectively; these agree well with the calculated values in Table II.

There are two weak features at 504.9 cm^{-1} and 512.9 cm^{-1} in the Tol-h_8 REMPI spectrum which require assignment, and a single feature appears in the Tol-d_3 REMPI spectrum at 501.3 cm^{-1}. Gascooke and Lawrance[44] have suggested that the lower wavenumber feature is associated with the $\mathscr{M}_{29}$ mode of the toluene-Ar complex, denoted $\overline{\mathscr{M}_{29}}$, which has been previously measured to have a redshift of 25 cm^{-1} (Ref. 24). If correct, we would expect a corresponding band in the Tol-d_3 spectrum at essentially the same shift: this fits very nicely the band at 501.3 cm^{-1}. The appearance of this feature in our mass-resolved spectrum is explained by the rapid vibrational predissociation as discussed by Da Campo and Mackenzie,[61] and referred to above, when discussing the Tol-h_8 band at 431.0 cm^{-1}.

The assignment of the 512.9 cm^{-1} band fits well with the expect wavenumber for the $\mathscr{M}_{11}(m = +3)$ band for Tol-h_8 and would be symmetry allowed; again, this fits with suggestions made by Gascooke and Lawrance.[44] As they note, it is interesting that the corresponding $m = +3$ band for the $\mathscr{M}_{19}\mathscr{M}_{20}$ combination band is not seen, and attribute this to the change in vibronic/torsional couplings in this region, compared to those in the region of the Fermi resonance at ~460 cm^{-1}. Given this assignment, it should be expected that a similar feature should be seen in the case of Tol-d_3. This would be expected at about 470 cm^{-1}, but there is nothing obvious in this wavenumber region, although there is a very weak feature at ~460 cm^{-1}; plausibly the expected feature is simply too weak to be observed in our work. A possible explanation for this weakness is that in Tol-h_8 the $\mathscr{M}_{11}(m = +3)$ transition gains some intensity by interaction with $\mathscr{M}_{29}$ (both of b_2 symmetry), while for Tol-d_3 this mechanism is not possible, since the $\mathscr{M}_{11}(m = +3)$ feature is now far removed from $\mathscr{M}_{29}$. Indeed, interaction of the $\mathscr{M}_{29}$ with $\mathscr{M}_{11}(m = +3)$ could partly explain the displaced m features mentioned above and in Ref. 44.

TABLE V. Bands in the $S_1 \leftarrow S_0$ transition below 700 cm^{-1} observed by REMPI spectroscopy.

	Wavenumber	
Assignment	Toluene-h_8	Toluene-d_3
[a]	165.1	155.3
$\mathscr{M}_{20}^{2}$	289.9	268.9
$\mathscr{M}_{30}$	331.4	294.6
$\mathscr{M}_{14}\mathscr{M}_{20}$	371.0	359.2
$\overline{\mathscr{M}_{11}}$	431.0	412.2
$\mathscr{M}_{14}^{2}$	451.8	452.4
$\mathscr{M}_{11}\ldots\mathscr{M}_{19}\mathscr{M}_{20}$	456.6	437.8
$\mathscr{M}_{19}\mathscr{M}_{20}\ldots\mathscr{M}_{11}$	462.2	443.0
$\mathscr{M}_{18}$ $(m = -3)$	472.6	436.0
$\mathscr{M}_{14}^{2}$ $(m = +3)$	...	480.6
$\overline{\mathscr{M}_{29}}$	504.9	501.3
$\mathscr{M}_{11}$ $(m = +3)$	512.9	...
$\mathscr{M}_{29}$	531.3	529.1
$\mathscr{M}_{14}\mathscr{M}_{19}$	539.3	530.5[b]
$\mathscr{M}_{19}^{2}$	628.5	612.3
$\mathscr{M}_{16}$	696.8	688.0

[a]Unassigned—see text.
[b]Shoulder.

We note that the $\mathscr{M}_{14}\mathscr{M}_{20}^{2}$ combination would have predicted values of 516 and 494 cm^{-1} for Tol-h_8 and Tol-d_3 respectively, which could be reasonably consistent with the 512.9 and 501.3 cm^{-1} features—but these are not symmetry-allowed under the C_{2v} point group, having a_2 symmetry, and so the above assignments appear to be the most likely. Finally, there is a weak feature at the far wavenumber end of the Tol-h_8 spectrum at 696.8 cm^{-1}, which has a corresponding feature at 688.0 cm^{-1} in the Tol-d_3 spectrum, a reasonable assignment of these bands is to $\mathscr{M}_{16}$ based on the calculated wavenumbers, which has b_1 symmetry and so is not symmetry allowed.

We summarize the observed REMPI bands and their assignments in Table V, and present the fundamental vibrational wavenumbers in Table VI—it is noted whether these are observed directly, or derived from combination/overtone bands. In Table VII we present a selection of the main ZEKE features with their assignments. In the text, further discussion on some of the weaker features, and the difficulties associated with their unequivocal assignment are given.

V. DISCUSSION

A. Comparison with time-resolved experiments

Very recent time-resolved experiments, focused on the Tol-h_8 Fermi resonance at 460 cm^{-1}, have been published by Davies *et al.*[41] In contrast to the present experiments, where a nanosecond laser is able to pick out single vibrational eigenstates (for the most part), in those experiments a picoseconds laser outputting a pulse with FWHM = 12–15 cm^{-1} and 1–2 ps was employed for both excitation and ionization. This

TABLE VI. Wavenumbers for fundamental vibrations of the S_1 state of Tol-h_8 and Tol-d_3.

		Fundamental Wavenumbers	
		Toluene-h_8	Toluene-d_3
A_1	$\mathscr{M}_{11}$	457[a]	438[a]
A_2	$\mathscr{M}_{14}$	226[b]	225[b]
B_1	$\mathscr{M}_{19}$	314[c]	306[c]
	$\mathscr{M}_{20}$	145[c]	134[c]
B_2	$\mathscr{M}_{29}$	531.6	529.6
	$\mathscr{M}_{30}$	331.4	294.6

[a]Perturbed value—fundamental observed in a Fermi resonance.
[b]Determined value derived from an observed combination band.
[c]Determined value derived from an observed overtone band.

means that the laser has the potential to excite a number of eigenstates coherently, forming a wavepacket. The constitution of the wavepacket depends on the number of eigenvalues covered by the form and energetic width of the laser pulse, convoluted with its intensity profile, together with the FCFs for each of the eigenstates. By delaying the ionization laser pulse with respect to the excitation laser pulse, then it is possible to probe the wavepacket at different times by detecting the time-dependent variation of the photoelectron spectrum onto which the wavepacket gets mapped, as a result of the instantaneous ionization event. In this way, providing the photoelectron spectra can be interpreted, the evolution of the wavepacket can be monitored. For example, if one identifies a single photoelectron band which has a strong time dependence, then one can obtain a good signal-to-noise variation of the intensity as a function of time. This time-dependent signal will be composed of a superposition of the contributions from each of the coherently excited eigenstates, whose population is determined by their FCFs and the picosecond pulse intensity at its energetic position. It is important to understand that the populations of the eigenstates do not vary with time: the time-dependent signal arises since the different eigenstates vibrate with different frequencies and are created with a phase difference between them, leading to time-dependent interference. It is the time variation of the instantaneous projection of the interference pattern onto a final state vibrational wavefunctions (those of the ionic state in Ref. 41), as deduced from the energies of the ejected photoelectrons, which is the observed time-dependent signal.

The simplest scenario is of two initial states (usually called zero-order states, ZOS) mixing to form the eigenstates, one of which is "bright" (optically active) and the other of which is "dark" (optically inactive), giving rise to two eigenstates, which will now each be optically active, with the activity carried by the "bright" zero-order state contribution in each case. Then, assuming there is a feature in the photoelectron spectrum that has different overall intensities from each eigenstate, the time-dependent signal will show oscillations in intensity caused by transitions from these two ZOSs, with a period, ω, determined by the separation of the two eigenstates ($\omega = \Delta E/\hbar$). At $t = 0$, the form of the combination of the eigenstates looks like one of the contributing zero-order states, and is sometimes referred to as the zero-order bright state, ZOB,[63] but it is important to note that the ZOB is *not* an eigenstate, it is merely the result of the superposition of the two actual eigenstates at $t = 0$. In this simplest picture, the other zero-order state is not seen at $t = 0$, and is often referred to as the zero-order dark state (ZOD). After the excitation, the wavepacket will evolve, as the two eigenstates vibrate out of phase, and at $t = 0$ it will look like the ZOB and at time π/ω it will look like the ZOD. If there are no other processes occurring to remove population from these eigenstates then,

TABLE VII. Band positions (cm^{-1}) relative to the origin of the $D_0^+ \leftarrow S_1$ transition for selected bands, using intermediate levels <700 cm^{-1} above the $S_1 \leftarrow S_0$ band origin, observed by ZEKE spectroscopy. The letters refer to the bands in the Fermi resonances, labelled in Figure 4. See text for details of assignments.

	Tol-h_8						Tol-d_3						
Intermediate	Origin	$\mathscr{M}_{30}$	A	B	C	$\mathscr{M}_{29}$	Origin	$\mathscr{M}_{30}$	E	F	G	H	$\mathscr{M}_{29}$
$\mathscr{M}_{14}$	335	335					334						
$\mathscr{M}_{30}$	342	342						303					
$\mathscr{M}_{30}(m_1{}^2)$		356											
$\mathscr{M}_{19}$	377												
$\mathscr{M}_{14}\mathscr{M}_{20}$						477							
$\mathscr{M}_{29}$						486							477
$\mathscr{M}_{11}$			496	496	496		475		473	473	471		
$\mathscr{M}_{29}(m_1^2)$						504							
$\mathscr{M}_{19}\mathscr{M}_{20}$	530			528	529				504	506	508		
$\mathscr{M}_{18}$	566							528					
$\mathscr{M}_{18}(m_0^{3-})$										540	542	542	
$\mathscr{M}_{14}^2$			669	669	669					667	670	666	
$\mathscr{M}_{14}\mathscr{M}_{19}$													703
$\mathscr{M}_{10}$	767						742						
$\mathscr{M}_{11}\mathscr{M}_{30}$		839						777					
$\mathscr{M}_8$	980			979	980								
$\mathscr{M}_{14}^3$												997	
$\mathscr{M}_{11}\mathscr{M}_{14}^2$												1139	

in principle, the time variation of the signal will continue ad infinitum, and energy will flow between the two ZOSs which make up the true eigenstates.

In reality, things can be more complicated, of course. So it may be that the eigenstates are made up of more than two ZOSs, and further that more than one may be bright and more than one may be dark. This can lead to the possibility that the ZOB may be composed of contributions of more than one ZOS. Now, of course, the time-dependent signal will be more complicated; however, assuming the time-dependent signal can be collected over a long enough time period with a good signal-to-noise ratio, which also relies on the populations of the eigenstates not being rapidly depleted by any mechanism, then the time-dependent signal can be Fourier-transformed, yielding the energy differences between the eigenstates which are contributing to the wavepacket.[63]

As mentioned above, Davies *et al.*[41] have investigated the time-dependent behavior observed in photoelectron spectra recorded *via* the toluene-h_8 S_1 intermediate levels comprising the Fermi resonance at around 460 cm^{-1}. As described in the previous paragraph, all of the optically active eigenstates within the width of the laser pulse are simultaneously excited, and these lead to a time-dependent signal being observed in the various photoelectron bands, dependent on the time delay between the excitation and ionization lasers. Early work by the Reid group in this wavenumber region[39] was limited by their then 200 cm^{-1} resolution; however, in this more recent work[41] they were able to make use of the slow-electron velocity-map imaging (SEVI) technique, obtaining a resolution of ~33 cm^{-1}, and so facilitating the monitoring of individual photoelectron features. In one set of experiments, the time evolution of the origin band in the photoelectron spectrum was monitored over 400 ps and the subsequent Fourier transform of the time-dependent signal in Ref. 41, revealed the presence of two Fourier components of 5.14 and 5.49 cm^{-1}. Note that the wavenumber resolution of the Fourier-transformed signal is significantly better than the band width of the picosecond laser, arising from conservation of the rotational quantum number between the coupled vibrational levels. The Fourier transform of the time-dependent signal from the $(\mathscr{M}_{14}^{2})^{+}$ band yielded a more-complicated picture, with five observed components at 4.92, 5.14, 5.49, 5.69, and 10.41 cm^{-1}. This immediately suggests that more than two eigenstates are contributing.

The subsequent assignment of a third contributing vibration as $\mathscr{M}_{14}^{2}$ ($16a^2$ in the Varsányi notation used in Ref. 41) was based upon the observation of a weak $\mathscr{M}_{14}^{2}$ band observed in the dispersed fluorescence spectrum of Hickman *et al.*[3] recorded *via* the S_1 0^0+457 cm^{-1} level and a band observed in the photoelectron spectra at the expected wavenumber for this vibration which displayed time-dependence. This would still not explain the five energy differences observed, and a consistent picture was eventually achieved by noting that the S_0 $m = 0$ and $m = 1$ internal rotor levels were both populated in the beam and each would lead to a set of vibronic transitions essentially degenerate within the wavenumber resolution of that work, and indeed the present work. However, owing to the wavenumber resolution achieved from the Fourier transformed time-dependent signals, these separations are resolved in Ref. 41, although one expected component was deduced not to have been observed. The eigenstates associated with the two m ladders can only create interference between themselves, and so the pattern is actually the sum of two separate interference patterns, and so both sets of eigenstate separations emerge upon Fourier transform.

The $m = 0$ states were assigned to the separations 4.92 cm^{-1}, 5.49 cm^{-1} and their sum, 10.41 cm^{-1}. These separations are consistent with our measured peak separations of features A, B, and C in the top trace of Figure 4 of 4.8 cm^{-1}, 5.6 cm^{-1}, and 10.4 cm^{-1}. Our resolution is not sufficient to resolve the other internal rotor levels, based on the closeness of the rotational constants in the S_0 and S_1 states;[31] however, these have been elegantly unraveled in the 2D-LIF work of Gascooke and Lawrance.[44] Again, it is remarkable, given the 15 cm^{-1} band width of the picosecond laser system used in Ref. 41, that these levels can be discerned from the time dependent signal, again suggesting strong rotational selectivity between the coupled rovibrational levels. The slightly different spacings for the $m = 0$ and $m = 1$ levels could be due to slightly different Fermi resonance interactions, and/or be due to other interactions which affect one set of the m levels more than the other; the 2D-LIF study of Gascooke and Lawrance[44] addresses this point explicitly, concluding that it is a combination of the two effects.

An involved analysis of the time-dependence of the deconvoluted bands in Ref. 41, coupled with a consideration of the laser pulse profile and some estimates/assumptions regarding the FCFs, allowed the deduction of the percentage contributions of the zero-order states to the eigenstates. They deduced that the level that gave rise to band B (termed eigenstate $|2\rangle$ therein) had a 52% contribution from $\mathscr{M}_{11}$ and with a 38% contribution from the $\mathscr{M}_{19}\mathscr{M}_{20}$ combination mode; while the level that gave rise to band C (labelled eigenstate $|1\rangle$ therein) had almost equal contributions from both of these modes (46% $\mathscr{M}_{11}$ and 53% $\mathscr{M}_{19}\mathscr{M}_{20}$). Davies *et al.*[41] report that the $\mathscr{M}_{14}^{2}$ zero-order state is only weakly coupled to the two other levels, with a 1% contribution to the eigenstate giving rise to band C, and a 10% contribution to the eigenstate giving rise to band B. $\mathscr{M}_{14}^{2}$ was concluded to be the dominant contribution to a third eigenstate (labelled $|3\rangle$ therein) which was composed of 2% $\mathscr{M}_{11}$, 9% $\mathscr{M}_{19}\mathscr{M}_{20}$ and 89% $\mathscr{M}_{14}^{2}$.

It is informative to compare these results with the ZEKE spectra. We have already noted that the $(\mathscr{M}_{14}^{2})^{+}$ state is far removed from the other two pertinent ionic states, and thus we would expect the contributions given above to be reflected in the ion band intensities, although these will be moderated by the FCFs. We see that the ZEKE spectrum for Tol-h_8 recorded via band A (corresponding to eigenstate $|3\rangle$ in Ref. 41) is dominated by the $(\mathscr{M}_{14}^{2})^{+}$ band, with only a very small contribution from $\mathscr{M}_{11}^{+}$, and no contribution from the $(\mathscr{M}_{19}\mathscr{M}_{20})^{+}$ combination band. This is slightly at odds with the derived contributions,[41] which suggest we should have observed the combination band since we see $\mathscr{M}_{11}^{+}$. When exciting via band C (corresponding to eigenstate $|1\rangle$ in Ref. 41), we see a dominance of the $(\mathscr{M}_{19}\mathscr{M}_{20})^{+}$ combination band, which is in line with the derived majority (52.6%) contribution from the $\mathscr{M}_{19}\mathscr{M}_{20}$ state in eigenstate $|1\rangle$; however, the band associated with $\mathscr{M}_{11}^{+}$ is weaker than might

be expected, given that $\mathscr{M}_{11}$ was deduced as contributing 46% to eigenstate $|1\rangle$. This behaviour is in line with the observed ZEKE spectrum obtained when exciting through band C (corresponding to eigenstate $|2\rangle$), here we would have expected the $\mathscr{M}_{11}^{+}$ band to be the most intense, as $\mathscr{M}_{11}$ is deduced to contribute 52% of eigenstate $|2\rangle$, whereas is actually less intense than the $(\mathscr{M}_{19}\mathscr{M}_{20})^{+}$ band even though the $\mathscr{M}_{19}\mathscr{M}_{20}$ state contributes 38%. We also note that, when exciting via band B, the $(\mathscr{M}_{14}^{2})^{+}$ band is more intense than one may have expected based on its derived 10% contribution to eigenstate $|2\rangle$. Possibly photoionization cross-section differences are an explanation for these observations, but ionic state mixing may also contribute. In the final stages of the writing of this paper, we learned of the 2D-LIF study of Gascooke and Lawrance,[44] in which they were also able to extract the eigenstate contributions in terms of the zero-order states. Those results give greater contributions of $\mathscr{M}_{14}^{2}$, in agreement with our ZEKE spectra observations.

Incidentally, the most intense feature in the ZEKE spectrum recorded via band B is the $(\mathscr{M}_{19}\mathscr{M}_{20})^{+}$ combination band at 529 cm^{-1}, and this is significantly different to the value of 515 cm^{-1} given for the same feature in Ref. 41, which barely overlaps with the value determined in the present work within the errors of both experiments. Since the 515 cm^{-1} value was obtained by deconvolution,[41] it is possible that this has led to this discrepancy; this might also suggest that separating the contributions to individual bands is an involved process.

We were particularly struck by the appearance of our REMPI spectrum for Tol-d_3, which has a very large contribution from the band H, compared to that of band A in Tol-h_8. Given its wavenumber separation from the other features, it would be expected that this would be less coupled to the other states than in Tol-h_8, and so be more "$\mathscr{M}_{14}^{2}$-like." That it is more intense seems to suggest that the $\mathscr{M}_{14}^{2}$ band carries oscillator strength, and is not reliant on intensity borrowing. It is unclear how this conclusion carries through to Tol-h_8. We note, however, that the $\mathscr{M}_{14}^{2}$ band does have a reasonable intensity at $t = 0$ ps as seen in Figure 4 of Ref. 41.

B. Comparison with fluorobenzene and chlorobenzene

1. REMPI spectra

Part of the impetus for our proposed new numbering scheme for the monosubstituted benzenes[1] was to be able to compare the trends in vibrations between species. The inconsistency of the other numbering schemes and how they were employed has led to a number of confusing assignments which do not appear to make sense when comparing between species, particularly those with "heavy" and "light" substituents, and we presented a consistent assignment of S_0 vibrations in Ref. 1. In Figure 6 we present the REMPI spectra of chlorobenzene, fluorobenzene, Tol-d_3, and Tol-h_8 arranged in order of mass. (We note that although corresponding spectra of bromobenzene have been reported,[64–66] these were not of sufficient clarity to include here for comparison; also, iodobenzene dissociates rapidly in the S_1 state.[64]) The

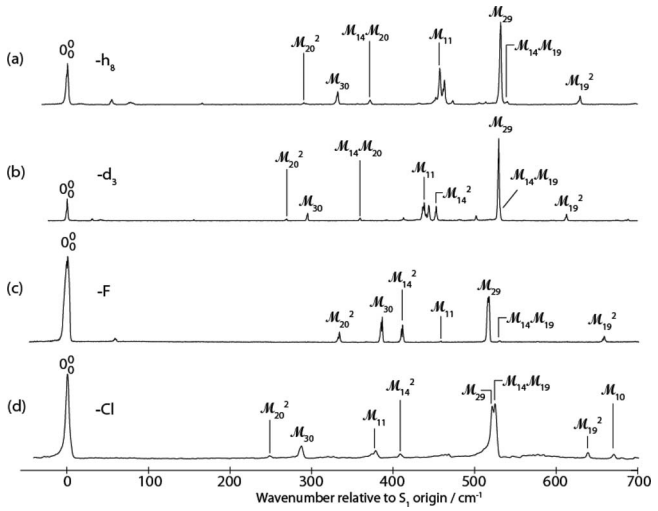

FIG. 6. (1 + 1) REMPI spectra of chlorobenzene, fluorobenzene, Tol-d_3, and Tol-h_8 in the range 0–700 cm^{-1}, see text for details. The spectrum for chlorobenzene has been taken from Ref. 67, while that for fluorobenzene is taken from Ref. 51; those for Tol-h_8 and Tol-d_3 are taken from the present work.

toluene spectra are both taken from the present work, the fluorobenzene spectrum was produced from the data used in Figure 1 of Ref. 51, and the chlorobenzene spectrum was produced from the data used in Figure 2 of Ref. 67. We have relabelled the assigned vibrations in terms of our $\mathscr{M}_i$ scheme, which sometimes implies a reassignment of a band based on Wilson/Varsányi nomenclature, although in reality the Wilson assignments were often not meaningful in any case. A brief glance indicates a high degree of consistency in the assignments, with the same vibrations consistently appearing with about the same relative intensity in each spectrum (although the laser intensity will be slowly varying across these regions); this is to be expected since the main electronic structure changes are within the phenyl ring. Where differences are seen that are not attributable solely to the change in reduced mass, these may be viewed as arising from substituent effects. We note that Walter *et al.*[66] present REMPI spectra of the lightest three halobenzenes, and these spectra also appear to show a good degree of similarity, particularly for chloro- and bromobenzene, where the wavenumber shifts, owing to the reduced mass, plateau.[1]

We initially note that there are general consistent features: $\mathscr{M}_{29}$ appears in all spectra relatively strongly, as well as weaker bands such as $\mathscr{M}_{30}$. The behaviour of the $\mathscr{M}_{11}$ is rather unusual for fluorobenzene, as it is very weak in that spectrum, whereas it would usually expected to be prominent, as it is in the other spectra (and in line with general observations on substituted benzenes). This has been rationalized for fluorobenzene from a very small change in geometry along the $\mathscr{M}_{11}$ coordinate during the $S_1 \leftarrow S_0$ transition.[51] Perhaps the two most striking observations are the double peak for chlorobenzene, attributed to a Fermi resonance in the S_1 state between $\mathscr{M}_{29}$ and $\mathscr{M}_{14}\mathscr{M}_{19}$ (see Ref. 67 and references therein), and this has also been confirmed in dispersed fluorescence studies by Imhof and Kleinermanns.[68] It may be noted that for both toluene isotopologues and for flu-

orobenzene, a small band to the blue of the main $\mathscr{M}_{29}$ band has also been assigned to the combination $\mathscr{M}_{14}\mathscr{M}_{19}$, but that the presence of a Fermi resonance is not obvious, suggesting that for chlorobenzene these features have moved into almost complete resonance. This supports the appearance of the ZEKE spectra recorded from each component of the double feature,[67] and is also in line with the results of the dispersed fluorescence study.[68] The ZEKE spectra exciting via the origin and $\mathscr{M}_{29}$ are discussed below.

Other striking observations are the presence of the very low wavenumber features for the toluene isotopologues, which are associated with the internal rotor levels of the methyl group; these are clearly not present for the two halobenzenes.

Finally, the analogue of the complicated Fermi resonances that appear in both Tol-h_8 and Tol-d_3 at ∼460 cm^{-1} is notable by its absence in the halobenzene cases, this is particularly notable for fluorobenzene since the difference in mass from Tol-d_3 is only a single mass unit. As discussed above, the Fermi resonance mostly arises as a result of interaction between the $\mathscr{M}_{11}$ and $\mathscr{M}_{19}\mathscr{M}_{20}$ vibrations. Previous work on monosubstituted benzenes, together with the time-resolved results of Davies *et al.*,[41] suggest that the $\mathscr{M}_{11}$ band should be "bright" and so be carrying the intensity of the Fermi resonance components. The lack of a Fermi resonance in fluorobenzene can therefore be attributed to the weak activity of $\mathscr{M}_{11}$ in this molecule (see above), so that even if $\mathscr{M}_{19}\mathscr{M}_{20}$ were in resonance, it still will not be seen as there is little intensity to borrow. In the case of chlorobenzene, we assume the $\mathscr{M}_{19}\mathscr{M}_{20}$ combination is not close enough to interact. These arguments go some way to explaining the observed activity of the Fermi resonance for the toluene isotopologues, but its complexity suggests the presence of more than just one interaction. In agreement with the work of Davies *et al.*[41] and the deductions from the present work and the 2D-LIF work by Gascooke and Lawrance,[44] the Fermi resonance is complicated further by interaction with the $\mathscr{M}_{14}^2$ combination band; additionally, Gascooke and Lawrance[44] have suggested further interaction with vibration-internal rotor combination bands. That the $\mathscr{M}_{14}^2$ band is not observed in resonance for fluorobenzene is explained both by the weakness of the $\mathscr{M}_{11}$ band, but also by the fact that $\mathscr{M}_{14}^2$ is more distant in wavenumber than for the toluene isotopologues. The other higher wavenumber feature $\mathscr{M}_{18}$ ($m = -3$) involves internal rotation and so clearly relies on the presence of the methyl group, and so it is clear this would be absent for the halobenzenes. That the $\mathscr{M}_{14}^2$ vibration has moved a reasonable amount between fluorobenzene and Tol-d_3 is consistent either with interaction between levels with contributions from internal rotation, or possibly that the $\mathscr{M}_{14}$ vibration in toluene itself has some internal rotation contribution.

In Figure 7 we show ZEKE spectra recorded via the vibrationless origin for the same selection of molecules. Again, the largely consistent assignment of features is noteworthy, with a dominance of bands assignable to totally symmetric vibrations. The signal-to-noise is somewhat better for the halobenzenes than for the toluene isotopologues, since the transition for the latter is very weak, as noted above. The appearance of the non-totally symmetric mode, $\mathscr{M}_{14}$ in all

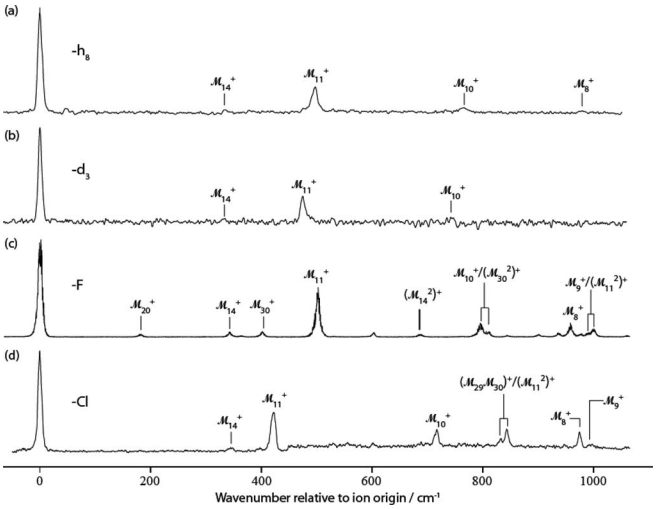

FIG. 7. $(1 + 1')$ ZEKE spectra of chlorobenzene, fluorobenzene, Tol-d_3, and Tol-h_8 when exciting through the 0^0 band, see text for details. The spectrum for chlorobenzene has been taken from Ref. 67, while that for fluorobenzene is taken from Ref. 51; those for Tol-h_8 and Tol-d_3 are taken from the present work.

four spectra is noteworthy. Fluorobenzene is slightly unusual in that there are bands seen arising from other additional non-totally symmetric bands in this region, $\mathscr{M}_{20}$ and $\mathscr{M}_{30}$, although these features are weak; we also note the much stronger $\mathscr{M}_{11}$ band here, compared to its very weak presence in the REMPI spectrum (see earlier in this subsection). It is interesting to note that in fluorobenzene and chlorobenzene, there are pairs of features seen towards the end of the scan which are close enough to suggest these may be in resonance; these also seem to result in the appearance of bands which are sharing intensity owing to their proximity.

In Figure 8, we show ZEKE spectra recorded via the $\mathscr{M}_{29}$ band, which has b_2 symmetry. It is noteworthy that now the spectrum is dominated by b_2 vibrations, in line with Franck-Condon factor expectations. We have noted that for this band in the S_1 state, the $\mathscr{M}_{14}\mathscr{M}_{19}$ combination band is in close proximity and leads to Fermi resonance for chlorobenzene. Hence the ZEKE spectrum shown is for the component which was deduced to have the greater percentage of $\mathscr{M}_{29}$ character.[67] Excitation via the main $\mathscr{M}_{29}$ feature for fluorobenzene leads to the appearance of $(\mathscr{M}_{14}\mathscr{M}_{29})^+$ in the ZEKE spectrum, suggesting that the latter and $\mathscr{M}_{29}^+$ states may be in resonance in the cation, as we have suggested for the toluene isotopologues. We note that in the fluorobenzene study,[51] there was difficulty in assigning the bands represented by β and 6b therein, based upon their simulated spectra, and it was suggested that these modes were mixed in the cation; in the present nomenclature the 6b vibration is $\mathscr{M}_{29}$ and we believe the β vibration is $\mathscr{M}_{30}$. The suggestion of mixing would be consistent with the ZEKE spectrum exciting via $\mathscr{M}_{29}$ gave rise to a double peak in the region of the $\Delta v = 0$ region (see Figure 8) as seen; however the experimentally determined fundamental wavenumbers of these vibrations have been shown to differ from the calculated values by ∼200 cm^{-1}. It is interesting to note that the assignment of the smaller peak to higher wavenumber is consistent with the

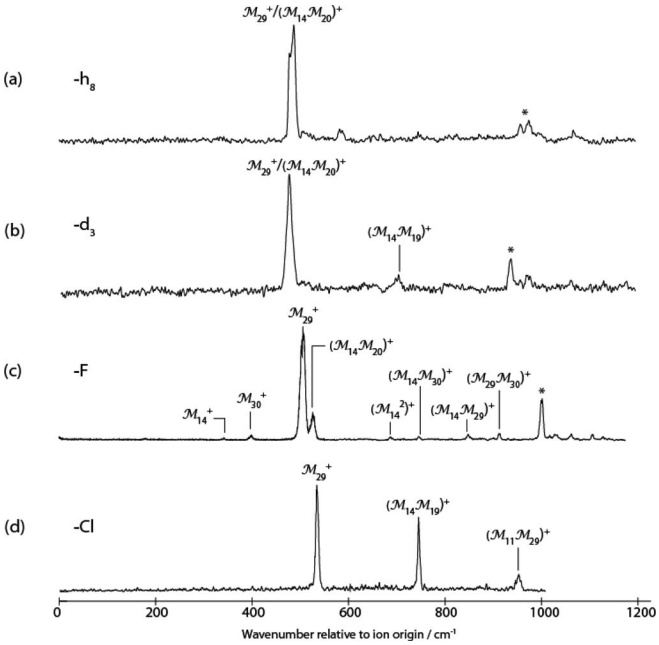

FIG. 8. $(1 + 1')$ ZEKE spectra of chlorobenzene, fluorobenzene, Tol-d_3, and Tol-h_8 when exciting through the $\mathscr{M}_{29}$ band, see text for details. The spectrum for chlorobenzene has been taken from Ref. 67, while that for fluorobenzene is taken from Ref. 51; those for Tol-h_8 and Tol-d_3 are taken from the present work.

assignment given in the present work. However, when exciting via $\mathscr{M}_{30}$ only a single band is seen at low wavenumber,[51] suggesting that any mixing between the $\mathscr{M}_{29}$ and $\mathscr{M}_{30}$ vibrations in the cation (or S_1 states) is minimal; a revisiting of the calculations may be instructive in this instance.

VI. CONCLUSIONS

We have presented the assignment of the vibrations of Tol-h_8 and Tol-d_3 in the S_0 state in terms of our $\mathscr{M}_i$ nomenclature,[1] based upon previous work. Although there was ambiguity in a couple of cases, generally the assignment of all of these vibrations seems secure. We then employed the results of one-colour REMPI spectroscopy to record the electronic excitation spectrum of the S_1 state of Tol-h_8 and Tol-d_3 below 700 cm^{-1}. The assignment of this spectrum was based on quantum chemical calculations and ZEKE spectra recorded through a number of these features, and making use of previous dispersed fluorescence results.[3] We also made use of quantum chemical results, via calculated harmonic vibrational wavenumbers for all three states involved, and also presenting anharmonic values for the S_0 and ground state cationic state. The assignment of most of the intense features was clear, but the complicated Fermi resonance, observed for both isotopologues, proved to be challenging. Fortuitously, we learned of work by Gascooke and Lawrance[44] during the final write-up of the present work, and that helped to confirm some of our hypotheses regarding this region of the spectrum, and provides new insight into other aspects of this feature. The summary is that, as well as the three main Fermi resonance contributions from $\mathscr{M}_{11}$, $\mathscr{M}_{19}\mathscr{M}_{20}$, and $\mathscr{M}_{14}^2$, as noted by Davies *et al.*[41] there are vibration-internal rotor interactions which cause shifting of the $m = 0$ and $m = 1$ ladders of states.[44] This assignment of the make-up of the Fermi resonance is consistent with the time-resolved study[41] and the analysis of the 2D-LIF[44] which initially was aimed at testing the hypothesis that two internal rotor ladders of states were contributing to the Fermi resonance. This hypothesis was confirmed, but further, the difference in spacing of these levels was attributed to interaction of the main Fermi resonance states with other vibration-torsion states. Our ZEKE spectra via the Fermi resonance components appear to be more consistent with the eigenstate composition suggested by Gascooke and Lawrance[44] than that reported by Davies *et al.*[41]

Finally, we compared REMPI and ZEKE spectra for the two toluene isotopologues with those for fluorobenzene and chlorobenzene, finding that the main activity was similar across the range, as expected. We discussed some of the differences, but particularly the absence of the complicated Fermi resonance for the two halobenzenes: a result that was surprising, since fluorobenzene and Tol-d_3 are only a mass unit apart, and so the vibrational frequencies might be expected to be close, if substituent effects are small. This observation was consistent with the complexity of the Fermi resonance arising largely from methyl internal rotation interactions, although wavenumber shifts and vibrational activity are also playing a role. We would like to note at this point that the $\mathscr{M}_i$ nomenclature helps tremendously in being able to ascertain correspondence between ring vibrations among different monosubstituted benzenes. Whilst it is true that there will be the occasional resonant mixing and substituent shifting of bands, our results[1] show that it seems to be possible still to identify "which vibration is which" in S_0; the present work suggests this is largely true for the S_1 state and cation (although the precise form of the vibration will alter, of course). Use of calculated artificial isotopic vibrational wavenumbers helps in this process, but also should allow the identification of significant substituent shifts, over and above simple reduced mass effects.

The present results mark a step change in our understanding of the spectroscopy of toluene and its cation; and the importance of the role that methyl internal rotation can have is noted, and particularly exemplified in the 2D-LIF paper of Gascooke and Lawrance.[44] We are currently preparing our work on the assignment of the higher wavenumber levels in toluene for publication.

ACKNOWLEDGMENTS

We are grateful for funding from the EPSRC (Grant No. EP/E046150/1) and for studentships to A. M. Gardner, A. M. Green, and V. M. Tamé-Reyes. We are particularly grateful to Warren Lawrance and Jason Gascooke (Flinders University, Adelaide, Australia) for sharing their results prior to publication, and highly insightful discussion, which has helped to shape aspects of the discussion in the present work, particularly with regard to the Fermi resonance. We are also grateful to Martin Cockett (University of York, UK) for discussion and sharing of original datafiles for fluorobenzene (reported in Ref. 51). Similarly, Stuart Mackenzie (University

of Oxford, UK) is thanked for his provision of datafiles published in Ref. 24, allowing us to check the appearance of the Fermi resonance feature in their work, and also to cross-check the wavenumber and appearance of the toluene-Ar bands. Katharine Reid is thanked for very useful discussions regarding the time-resolved experiments.

[1]A. M. Gardner and T. G. Wright, J. Chem. Phys. **135**, 114305 (2011).
[2]G. Varsányi, *Assignments of the Vibrational Spectra of Seven Hundred Benzene Derivatives* (John Wiley and Sons, New York, 1974), Vol. I.
[3]C. G. Hickman, J. R. Gascooke and W. D. Lawrance, J. Chem. Phys. **104**, 4887 (1996).
[4]K. S. Pitzer and D. W. Scott, J. Am. Chem. Soc. **65**, 803 (1943).
[5]J. K. Wilmshurst and H. J. Bernstein, Can. J. Chem. **35**, 911 (1957).
[6]N. Fuson, C. Garrigou-Lagrange, and M. L. Josien, Spectrochim. Acta **16**, 106 (1960).
[7]C. La Lau and R. G. Snyder, Spectrochim. Acta. A **27**, 2073 (1971).
[8]G. Varsányi, *Assignments for Vibrational Spectra of Seven Hundred Benzene Derivatives* (Wiley, New York, 1974), Vol. II.
[9]A. M. Bogomolov, Opt. Spectrosc. **9**, 162 (1960).
[10]J. A. Draeger, Spectrochim. Acta A **41**, 607 (1985).
[11]M. Tasumi, T. Urano, and M. Nakata, J. Mol. Struct. **146**, 383 (1986).
[12]L. M. Sverdlov, M. A. Kovner, and E. P. Krainov, *Vibrational Spectra of Polyatomic Molecules* (Wiley, New York, 1973).
[13]V. J. Morrison and J. D. Laposa, Spectrochim. Acta, Part A **32**, 443 (1976).
[14]N. Ginsburg, W. W. Robertson, and F. A. Matsen, J. Chem. Phys. **14**, 511 (1946).
[15]J. Savard, Ann. Chim. (Paris) **11**, 287 (1929).
[16]K. Masaki, Bull. Chem. Soc. Jpn. **11**, 346 (1936).
[17]H. Sponer, J. Chem. Phys. **10**, 672 (1942).
[18]J. Kahane-Paillous and S. Leach, J. Chim. Phys. Phys.-Chim. Biol. **55**, 439 (1958).
[19]R. Vasudev and J. C. D. Brand, Chem. Phys. **37**, 211 (1979).
[20]K. Krogh-Jespersen, R. P. Rava, and L. Goodman, Chem. Phys. **44**, 295 (1979).
[21]W. J. Balfour and Y. Fried, Can. J. Phys. **72**, 1218 (1994).
[22]W. J. Balfour and R. S. Ram, Can. J. Phys. **72**, 1225 (1994).
[23]M. Schauer, K. Law, and E. R. Bernstein, J. Chem. Phys. **81**, 49 (1984).
[24]R. J. Doyle, E. S. J. Love, R. Da Campo, and S. R. Mackenzie, J. Chem. Phys. **122**, 194315 (2005).
[25]C. G. Eisenhardt and H. Baumgärtel, Ber. Bunsenges. Phys. Chem. **102**, 1803 (1998).
[26]P. J. Breen, J. A. Warren, E. R. Bernstein, and J. I. Seeman, J. Chem. Phys. **87**, 1917 (1987).
[27]J. Murakami, M. Ito, and K. Kaya, Chem. Phys. Lett. **80**, 203 (1981).
[28]R. A. Walker, E. Richard, K.-T. Lu, E. L. Sibert III, and J. C. Weisshaar, J. Chem. Phys. **102**, 8718 (1995).
[29]N. Kanamaru, Chem. Phys. Lett. **363**, 435 (2002).
[30]A. L. L. East, H. Liu, E. C. Lim, P. Jensen, I. Déchène, M. Z. Zgierski, W. Siebrand, and P. R. Bunker, J. Chem. Phys. **112**, 167 (2000).
[31]D. R. Borst and D. W. Pratt, J. Chem. Phys. **113**, 3658 (2000).
[32]K. Watanabe, J. Chem. Phys. **22**, 1564 (1954).
[33]K. Watanabe, T. Nakayama, and J. Mottl, J. Quant. Spectrosc. Radiat. Transf. **2**, 369 (1962).
[34]T. P. Debies and J. W. Rabalais, J. Electron Spectrosc. Relat. Phenom. **1**, 355 (1972).
[35]J. T. Meek, S. R Long, and J. P. Reilly, J. Phys. Chem. **86**, 2809 (1982).
[36]D. A. Shaw, D. M. P. Holland, M. A. MacDonald, M. A. Hayes, L. G. Shpinkova, E. E. Rennie, C. A. F. Johnson, J. E. Parker, and W. von Niessen, Chem. Phys. **230**, 97 (1998).
[37]P. T. Whiteside, A. K. King, and K. L. Reid, J. Chem. Phys. **123**, 204316 (2005).
[38]P. T. Whiteside, A. K. King, J. A. Davies, and K. L. Reid, J. Chem. Phys. **123**, 204317 (2005).
[39]C. J. Hamond, K. L. Reid, and K. L. Ronayne, J. Chem. Phys. **124**, 201102 (2006).
[40]E. Fermi, Z. Phys. **71**, 250 (1931).
[41]J. A. Davies, A. M. Green, and K. L. Reid, Phys. Chem. Chem. Phys. **12**, 9872 (2010).
[42]K. T. Lu, G. C. Eiden, and J. C. Weisshaar, J. Phys. Chem. **96**, 9742 (1992).
[43]F. Gunzer and J. Grotemeyer, Phys. Chem. Chem. Phys. **4**, 5966 (2002).
[44]J. R. Gascooke and W. D. Lawrance, J. Chem. Phys. **138**, 134302 (2013).
[45]S. D. Gamblin, S. E. Daire, J. Lozeille, and T. G. Wright, Chem. Phys. Lett. **325**, 232 (2000).
[46]C. J. Hammond, V. L. Ayles, D. E. Bergeron, K. L. Reid, and T. G. Wright, J. Chem. Phys. **125**, 124308 (2006).
[47]V. L. Ayles, C. J. Hammond, D. E. Bergeron, O. J. Richards, and T. G. Wright, J. Chem. Phys. **126**, 244304 (2007).
[48]A. R. Bacon and J. M. Hollas, Faraday Discuss. Chem. Soc. **86**, 129 (1988).
[49]M. J. Frisch, G. W. Trucks, H. B. Schlegel *et al.*, GAUSSIAN 09, Revision A.02, Gaussian, Inc., Wallingford, CT, 2009.
[50]I. Pugliesi and K. Müller-Dethlefs, J. Phys. Chem. A **110**, 4657 (2006), see http://www.fclab2.net/.
[51]I. Pugliesi, N. M. Tonge, and M. C. R. Cockett, J. Chem. Phys. **129**, 104303 (2008).
[52]A. Bolvinos, J. Philis, E. Pantos, P. Tsekeris, and G. Andritsopoulos, J. Mol. Spectrosc. **94**, 55 (1982).
[53]D. M. Haaland and G. C. Nieman, J. Chem. Phys. **59**, 4435 (1973).
[54]J. E, Hopkins, D. E. Powers, and R. E. Smalley, J. Chem. Phys. **72**, 5039 (1980).
[55]Z.-Q. Zhao, C. S. Parmenter, D. B. Moss, A. J. Bradley, A. E. W. Knight, and K. G. Owens, J. Chem. Phys. **96**, 6362 (1992).
[56]H. D. Rudolph, H. Dreizler, A. Jaeschke, and P. Wendling, Z. Naturforsch. A **22a**, 940 (1967).
[57]W. A. Kreiner, H. D. Rudolph, and B. T. Tan, J. Mol. Spectrosc. **48**, 86 (1973).
[58]V. Abir-Ebrahimi, A. Choplin, J. Demaison, and G. Roussey, J. Mol. Spectrosc. **89**, 42 (1981).
[59]A. Musgrave and T. G. Wright, J. Chem. Phys. **122**, 074312 (2005).
[60]See, for example, G. Reiser, D. Rieger, T. G. Wright, K. Müller-Dethlefs, and E. W. Schlag, J. Phys. Chem. **97**, 4335 (1993).
[61]R. Da Campo and S. R. Mackenzie, Chem. Phys. Lett. **452**, 6 (2008).
[62]B. T. Darling and D. M. Dennison, Phys. Rev. **57**, 128 (1940).
[63]D. J. Nesbitt and R. W. Field, J. Phys. Chem. **100**, 12735 (1996).
[64]T. G. Dietz, M. A. Duncan, M. G. Liverman, and R. E. Smalley, J. Chem. Phys. **73**, 4816 (1980).
[65]U. Boesl, R. Zimmermann, C. Weickhardt, D. Lenoir, K.-W. Schramm, A. Kettrup, and E. W. Schlag, Chemosphere **29**, 1429 (1994).
[66]K. Walter, K. Scherm, and U. Boesl, J. Phys. Chem. **95**, 1188 (1991).
[67]T. G. Wright, S. I. Panov, and T. A. Miller, J. Chem. Phys. **102**, 4793 (1995).
[68]P. Imhof and K. Kleinermanns, Chem. Phys. **270**, 227 (2001).